



Key Points:

- Venus's seismogenic thickness is estimated from geophysics and geodynamics, using the 600°C isotherm as a proxy
- Across the planet, the depth of the 600°C isotherm typically varies between 2 and 35 km
- The presence of intrusive magmatism locally decreases the thickness of the seismogenic layer

Supporting Information:

Supporting Information may be found in the online version of this article.

Correspondence to:

J. S. Maia,
julia.maia@dlr.de

Citation:

Maia, J. S., Plesa, A.-C., van Zelst, I., Ghail, R., Gülcher, A. J. P., Panning, M. P., et al. (2025). The seismogenic thickness of Venus. *Journal of Geophysical Research: Planets*, 130, e2025JE009065. <https://doi.org/10.1029/2025JE009065>

Received 1 MAR 2025

Accepted 9 JUN 2025

Author Contributions:

Conceptualization: Julia S. Maia, Ana-Catalina Plesa, Iris van Zelst, Richard Ghail

Data curation: Julia S. Maia, Ana-Catalina Plesa

Formal analysis: Julia S. Maia, Ana-Catalina Plesa

Funding acquisition: Ana-Catalina Plesa, Iris van Zelst

Investigation: Julia S. Maia, Ana-Catalina Plesa

Methodology: Julia S. Maia, Ana-Catalina Plesa










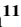


Project administration: Iris van Zelst

Software: Julia S. Maia, Ana-Catalina Plesa

Visualization: Julia S. Maia, Ana-Catalina Plesa, Iris van Zelst

Writing – original draft: Julia S. Maia, Ana-Catalina Plesa

The Seismogenic Thickness of Venus

Julia S. Maia¹ , Ana-Catalina Plesa¹ , Iris van Zelst^{1,2,3} , Richard Ghail⁴ , Anna J. P. Gülcher⁵ , Mark P. Panning⁶ , Sven Peter Näsholm^{7,8} , Barbara De Toffoli⁹, Anna C. Horleston¹⁰ , Krystyna T. Smolinski¹¹ , Sara Klaasen¹¹ , Robert R. Herrick¹² , and Raphael F. Garcia¹³ 

¹Institute of Space Research, German Aerospace Center (DLR) Berlin, Berlin, Germany, ²Centre of Astronomy and Astrophysics, Technical University of Berlin, Berlin, Germany, ³Now at: School of GeoSciences, University of Edinburgh, Edinburgh, UK, ⁴Department of Earth Sciences, Royal Holloway, University of London, Egham, UK, ⁵Center for Space and Habitability, University of Bern, Bern, Switzerland, ⁶Jet Propulsion Laboratory, California Institute of Technology, Pasadena, CA, USA, ⁷Department of Informatics, University of Oslo, Oslo, Norway, ⁸NORSAR, Kjeller, Norway, ⁹Department of Geosciences, University of Padova, Padova, Italy, ¹⁰School of Earth Sciences, University of Bristol, Bristol, UK, ¹¹Department of Earth and Planetary Sciences, ETH Zürich, Zürich, Switzerland, ¹²Institute of Northern Engineering, University of Alaska Fairbanks, Fairbanks, AK, USA, ¹³Institut Supérieur de l'Aéronautique et de l'Espace ISAE-SUPAERO, Université de Toulouse, Toulouse, France

Abstract Growing evidence that volcanism is currently ongoing on Venus suggests that the sister planet of the Earth may also be seismically active. Given the success of seismic measurements on Mars and the Moon to reveal the interior structure of these bodies, seismic investigations on Venus are a natural next step. The potential for seismic activity is closely linked to the thickness of the so-called seismogenic layer, that is, the region where rocks behave in a brittle manner and quakes can nucleate. On Earth, the seismogenic thickness is correlated with the thermal structure of the lithosphere, and is typically associated with the depth of the 600°C isotherm. Here, we combine geophysical constraints with thermal evolution models to estimate the thermal structure of Venus' lithosphere and determine the corresponding seismogenic thickness. Taking all estimates into account, our results show that the seismogenic thickness overall varies from 2 to 35 km. The lowest values are associated with areas that probably correspond to local thermal anomalies associated with magmatic processes. This interpretation is corroborated by geodynamic models, which show that intrusive magmatism can largely increase the temperature within the lithosphere at local scales. The seismogenic layer is thickest at volcanic plains which are commonly associated with regions of mantle downwellings. In these regions, the seismogenic layer likely reaches Venus' mantle, while in areas with a thick crust or anomalously high thermal gradients, quakes might be limited to the crust. Our study provides evidence that Venus has a substantial seismic potential.

Plain Language Summary Without plate tectonics, Venus was generally thought to have low geological activity, similar to stagnant-lid planets like Mars. However, evidence of ongoing volcanism suggests that Venus is geologically active today. Geological processes, such as tectonics and volcanism, are closely tied to seismicity. Investigating a planet's seismicity is a direct approach to measuring its geological activity levels while providing fundamental constraints of its deep interior. Seismology has revolutionized our knowledge about the Moon, Mars, and Earth, and a seismic-focused mission to Venus is a natural next step to explore the interior of our neighbor planet. To evaluate Venus' seismic potential, we determine the thickness of the seismogenic layer—the region where rocks break and release seismic energy. We use constraints from gravity and topography data and geodynamic models to estimate the thermal structure of Venus' subsurface, allowing for an indirect estimate of its seismogenic thickness. Our results show that Venus' seismogenic thickness varies spatially, from less than 10 km at rift zones and mantle upwelling regions to over 30 km within regions typically associated with cold mantle downwellings. Overall, this study supports the hypothesis that Venus has vast potential for seismicity, at depths comparable to those observed for quakes on Earth.

1. Introduction

The surface of Venus presents a large variety of tectonic structures, even in the absence of Earth-like plate tectonics. These include, but are not limited to, major rift zones that extend for thousands of kilometers (e.g., Ivanov & Head, 2011), hundreds of circular volcano-tectonic structures called coronae, some of which may be

Writing – review & editing: Julia S. Maia, Ana-Catalina Plesa, Iris van Zelst, Richard Ghail, Anna J. P. Gülcher, Mark P. Panning, Sven Peter Näsholm, Barbara De Toffoli, Anna C. Horleston, Krystyna T. Smolinski, Sara Klaasen, Robert R. Herrick, Raphael F. Garcia

associated with regional subduction (Cascioli et al., 2025; Davaille et al., 2017; Sandwell & Schubert, 1992; Stofan et al., 1992), and tens of thousands of wrinkle ridges related to compressive stresses (Bilotti & Suppe, 1999; Sabbeth et al., 2023). The heavily deformed surface also hosts at least 85,000 volcanic edifices (Hahn & Byrne, 2023). Precise ages for the formation of these features are not well known, but crater statistics suggest that Venus' surface is relatively young and uniform in age, around 250–800 Myr old (Herrick et al., 2023; Le Feuvre & Wiczorek, 2011). More importantly, a growing number of studies provide observational evidence that Venus is volcanically active today (Herrick & Hensley, 2023; Smrekar et al., 2010; Sulcanese et al., 2024). Therefore, it is plausible, or even likely, to consider that Venus is also a seismically active planet.

Currently, we have very limited knowledge about the seismicity of Venus, mostly due to the lack of seismic data. However, the recent evidence for present-day geological activity on the planet, along with the development of new seismic wave detection methods that could be applied to Venus (e.g., Brissaud et al., 2021; Garcia et al., 2024; Krishnamoorthy & Bowman, 2023), and the broad success of the InSight Mission to Mars (e.g., Banerdt et al., 2020) are triggering a growing interest in Venus' seismicity and the potential for seismology-focused missions in the future. In this context, it is highly valuable to have first-order assessments of the seismological properties of the planet, which can be obtained by combining geophysical constraints and models for Venus with knowledge extrapolated from the Earth and other terrestrial planets (Van Zelst et al., 2024).

A key factor in characterizing a planet's seismicity is the thickness of its seismogenic layer—the outer, brittle portion where quakes can nucleate. This depth typically marks the lower boundary of seismic activity, directly influencing a planet's potential for quakes. In addition, the thermal properties of this layer strongly affect the shear modulus of rocks which, in turn, has implications regarding the seismic moment, and hence magnitude, of possible quakes (e.g., England, 2018). Constraints on the depth of earthquakes, modeling studies, and laboratory experiments suggest a strong correlation between the maximum depth of seismic events and the temperature structure of Earth's lithosphere (McKenzie et al., 2005; Scholz, 1998). Hence, drawing a parallel between Earth and Venus, it is possible to use the current knowledge of Venus' thermal structure to estimate the seismogenic thickness of the planet.

In a recent study, Van Zelst et al. (2024) used end-member lithospheric thermal gradient estimates from earlier works (Bjornnes et al., 2021; Smrekar et al., 2023) to derive global upper and lower bounds on the seismogenic thickness of Venus. These values were then used to obtain estimates of Venus' current seismicity based on scaling Earth's seismicity to Venus via tectonic analogs for various proposed levels of tectonic activity (Van Zelst et al., 2024). This first-order approximation towards seismogenic thickness is a useful simplification in their study to obtain global upper and lower bound estimates of seismicity, but it neglects the inherent 3-D component (i.e., lateral variation) of seismogenic thickness that we know to exist on Earth. In this study, we therefore provide the first comprehensive global assessment of seismogenic thickness using direct constraints from topography and gravity data and geodynamic models. As such, we perform an in-depth analysis of the thermal structure of Venus' lithosphere to obtain the first global, laterally varying seismogenic thickness maps of Venus.

The outline of this paper is as follows. Section 2 describes how we estimate the seismogenic thickness from lithospheric thermal gradient profiles and discusses the assumptions involved. Then, we present the three individual but correlated analyses we perform to estimate Venus' seismogenic thickness: (a) compilation of elastic thickness estimates from previous lithospheric flexure studies (Section 3); (b) geodynamic modeling for different magmatic styles (Section 4); and (c) mantle density anomalies constraints from gravity-topography investigations (Section 5). In Section 6 we present a comparison between the different estimates and discuss the relation between temperature and brittle rheological behavior. Concluding remarks and perspectives regarding future seismicity-focused missions to Venus are presented in Section 7.

2. From Temperature to Seismogenic Thickness

The most accurate way of defining the depth of the seismogenic layer of a planet is by detecting a large number of quakes with seismometers and constraining their depths, allowing for the determination of the maximum depth at which they typically happen, and hence the seismogenic thickness. When it comes to planetary sciences, however, we commonly do the reverse: understand the mechanical properties of the lithosphere using different geophysical approaches to map the seismogenic thickness variations and help determine optimal locations to send seismic instruments in the future (Garcia et al., 2024; Stevenson et al., 2015; Van Zelst et al., 2024).

Combining thermal modeling studies with precise earthquake localization efforts for the Earth has shown that the depth of the seismogenic layer, which is the layer where quakes can nucleate, is closely related to the temperature structure of the lithosphere (e.g., Craig et al., 2014; McKenzie et al., 2005; F. Richards et al., 2018; Van Zelst et al., 2023). In other words, the maximum depth at which earthquakes can nucleate is closely related to a temperature threshold T_{seis} . Therefore, by estimating lithospheric thermal gradients (dT/dz), one can compute the associated seismogenic thickness d_{seis} if T_{seis} is known, using:

$$d_{\text{seis}} = \frac{T_{\text{seis}} - T_{\text{surface}}}{dT/dz}, \quad (1)$$

where T_{surface} is the surface temperature (464°C for Venus).

Since there are no direct constraints for T_{seis} on Venus, the most reasonable approach is to adapt the knowledge derived from Earth to the context of Venus. For Earth's oceanic lithosphere, there is a consistent monotonic increase of the maximum quake depth with the age (hence steady cooling) of a tectonic plate. According to thermal models and surface heat flow constraints, the maximum observed focal depths correspond to a cutoff temperature of 600°C in the oceanic lithosphere, which is typically located in Earth's upper mantle (e.g., Jackson et al., 2008; Lucazeau, 2019; McKenzie et al., 2005). For continental lithosphere, this relation is not as straightforward. In many places, earthquakes are limited to the upper crust (10–20 km depth), where temperatures typically reach 350°C (e.g., Jackson et al., 2008; Zuza & Cao, 2020). This difference can be mostly explained by the weaker rheology of continental crust due to a commonly hydrated and felsic composition. Nevertheless, deeper quakes, reaching the lower crust and potentially uppermost mantle, have been observed in several continental regions on Earth, such as the Baikal Rift, the East African Rift and the Himalayas (e.g., Craig et al., 2012; Craig & Jackson, 2021; Déverchère et al., 2001; Jackson et al., 2008). These measurements show that, in some portions of continental lithosphere, quakes can also occur at temperatures of 500 to over 600°C, which suggests that at least the lower crust must be composed of an anhydrous, probably mafic, composition in these regions (Albaric et al., 2009; Craig & Jackson, 2021; Déverchère et al., 2001).

Given that Venus' crust is primarily basaltic (e.g., Basilevsky & Head, 2003; Surkov et al., 1984; Surkov et al., 1986) and the lithosphere is often argued to be governed by a dry rheology (e.g., Foster & Nimmo, 1996; Kaula, 1990; Kohlstedt & Mackwell, 2009; Nimmo & Mackwell, 2023), we believe that the use of the 600°C isotherm to define the thickness of the seismogenic layer is a reasonable, first-order approximation for both crust and mantle. Hence, in this study, we will use the depth of the 600°C as a proxy to calculate the seismogenic thickness. Nevertheless, one cannot neglect the uncertainties of temperature estimates for the Earth, nor the influence of other parameters that can effect the thickness of the seismogenic layer—such as strain rate, frictional regime, pressure, hydration, and presence of glass in basaltic rocks (e.g., Violay et al., 2012). Hence, for completeness we also calculate the seismogenic thickness of Venus assuming the 500°C and 800°C isotherms as temperature thresholds (see Figure S6 in Supporting Information S1). The reasoning behind the choice of these values and their associated seismogenic thickness estimates are discussed in Section 6. Note that in Sections 3–5, we present our main results only in terms of our reference isotherm of 600°C, for simplicity.

3. Seismogenic Thickness Estimates From Flexure

A well-established method to investigate the thermal properties of terrestrial planets is estimating the thickness of the elastic lithosphere using flexural loading models. The basic principle is that high-elevation geological features act as loads on the surface, causing the lithosphere to bend downwards (Turcotte et al., 1981). The amount of deflection correlates with lithospheric thickness: the thicker the lithosphere, the more rigid it is, and the less it will deflect in the presence of a load. This process is typically modeled assuming the lithosphere behaves as a thin elastic shell. Although simple, this approach is useful because it results in an analytical model, allowing for the investigation of large parameter spaces. The lithospheric deflection is controlled by the so-called flexural rigidity, which depends on the elastic shell thickness, commonly referred to as elastic thickness (see, e.g., Beuthe, 2008; Turcotte et al., 1981, for a formal definition). In turn, the elastic thickness is closely related to the lithospheric thermal structure and can be used to constrain the lithospheric thermal gradient (McNutt, 1984).

Several studies have used elastic thickness estimates to better understand the thermal state of Venus. Some of them (e.g., Borrelli et al., 2021; O'Rourke & Smrekar, 2018; Russell & Johnson, 2021; Sandwell &

Schubert, 1992; Smrekar et al., 2023; Solomon & Head, 1990) investigated the deflection in topography, characterized by a flexural bulge, around loads from several rifts, coronae, and steep-sided domes. Other studies combined gravity and topography data to estimate the elastic thickness of large features such as volcanic rises and crustal plateaus (Anderson & Smrekar, 2006; Jimenez-Diaz et al., 2015; Maia & Wiczorek, 2022; Phillips et al., 1997; Simons et al., 1997; Smrekar, 1994). These analyses used spectral admittance (i.e., the wavelength-dependent ratio between gravity and topography) to constrain the interior structure of geological features by comparing observed admittance with those predicted by flexural models. Studies using only topography data have the main advantage of being able to investigate relatively small structures, on the order of tens of kilometers, while gravity investigations are limited to features larger than a few hundred kilometers due to the low spatial resolution of Venus' gravity data (Konopliv et al., 1999). However, gravity-topography analyses can provide additional constraints on interior structure, such as the crustal thickness. Moreover, the topographic signature of deflection is often masked by geological processes, such as later infill by lava flows (McGovern & Solomon, 1997), limiting the topographic methods.

Here, we compile a database of Venus elastic thickness estimations from previous works, selecting studies that include information on plate curvature, as this is essential to derive lithospheric thermal gradients. Our final database includes local elastic thickness values by Phillips et al. (1997), O'Rourke and Smrekar (2018), Borrelli et al. (2021), Maia and Wiczorek (2022), Smrekar et al. (2023). From these data, we compute the lithospheric thermal gradient using the moment matching technique by McNutt (1984) with the code developed by Broquet et al. (2020). The conversion from elastic thickness to mechanical thickness requires assumptions regarding the strain rate and rheological parameters, which are not well-constrained for Venus. We assume a strain rate of 10^{-16} s^{-1} and a dry diabase rheology with parameters derived from the study by Mackwell et al. (1998). We use a minimum differential stress of 50 MPa to limit the mechanical lithosphere, as in McNutt (1984). Although many of these studies performed thermal gradient estimates, we chose to recalculate all of them with the same set of parameters for consistency.

Figure 1 presents the spatial distribution of elastic thickness and associated seismogenic thickness constraints on Venus. Elastic thickness estimates range from 1.2 to 45.0 km, with a median of 9.7 km and a mean of 11.7 km, while the seismogenic thickness ranges from 1.5 to 102.0 km with a median of 10.0 km and a mean of 12.8 km. The maps reveal relatively high variability in the seismogenic (and elastic) thickness estimates over short spatial scales and also highlight some regional trends. Parga Chasma and Lada Terra appear to be associated with thin seismogenic thicknesses (medians of 6.7 and 5.8 km, respectively), while the Diana-Dali Chasma region and the Tellus Regio surroundings have generally larger values (medians of 15.3 and 14.0 km, respectively). Moreover, as discussed in Maia and Wiczorek (2022), the thin elastic (and seismogenic) thickness of plateaus may indicate that these features are remnants from an ancient, hotter period, not representing the current thermal state of the regions. Overall, most of the elastic thickness estimates are intrinsically associated with magmatic and/or hotspot regions, which likely bias the estimated median towards high thermal gradients. We note that our thermal gradient estimates are very similar, although not exactly the same as the results presented in previous studies using moment matching technique (e.g., Borrelli et al., 2021; O'Rourke & Smrekar, 2018; Smrekar et al., 2023). These discrepancies are mainly attributed to differences in the choice of parameters when doing the elastic thickness to mechanical thickness conversion, such as the rheology parameters derived from different laboratory experiments.

To better quantify the variations of the seismogenic thickness constraints due to the choice of poorly constrained parameters, we performed a range of sensitivity tests, summarized in Figure 2. We estimated the seismogenic thickness considering different sets of (a) surface temperature, (b) strain rates, and (c) rheological parameters, while panel (d) shows seismogenic thickness estimates derived from the base of the brittle layer. Using surface temperature ranges from the Venus Climate Database (Lebonnois et al., 2016), we find that the surface temperature has a negligible impact on the seismogenic thickness estimates for most of the planet's surface. Only in a few highly elevated regions, such as Atla, Beta, Ovda and Ishtar Terra, this property starts having an impact. For example, for surface temperatures of 700 K (above ~ 4 km altitude) the median seismogenic thickness reduces by 14% (8.6 km). The strain rate, which is poorly constrained on Venus, has a more significant effect. On Earth, actively deforming areas have a representative strain rate of 10^{-14} – 10^{-15} s^{-1} (Fagereng & Biggs, 2019; Pfiffner & Ramsay, 1982) and geodetic measurements indicate that strain rates range from 10^{-13} to 10^{-17} s^{-1} globally (Kreemer et al., 2014). On Venus, estimates from crater deformation suggest global average values of around 10^{-17} s^{-1} (Grimm, 1994), while regions of high deformation could reach strain rates above 10^{-15} s^{-1} (Brown & Grimm, 1997). For our reference estimates, we chose a strain rate of 10^{-16} s^{-1} which represents an intermediate

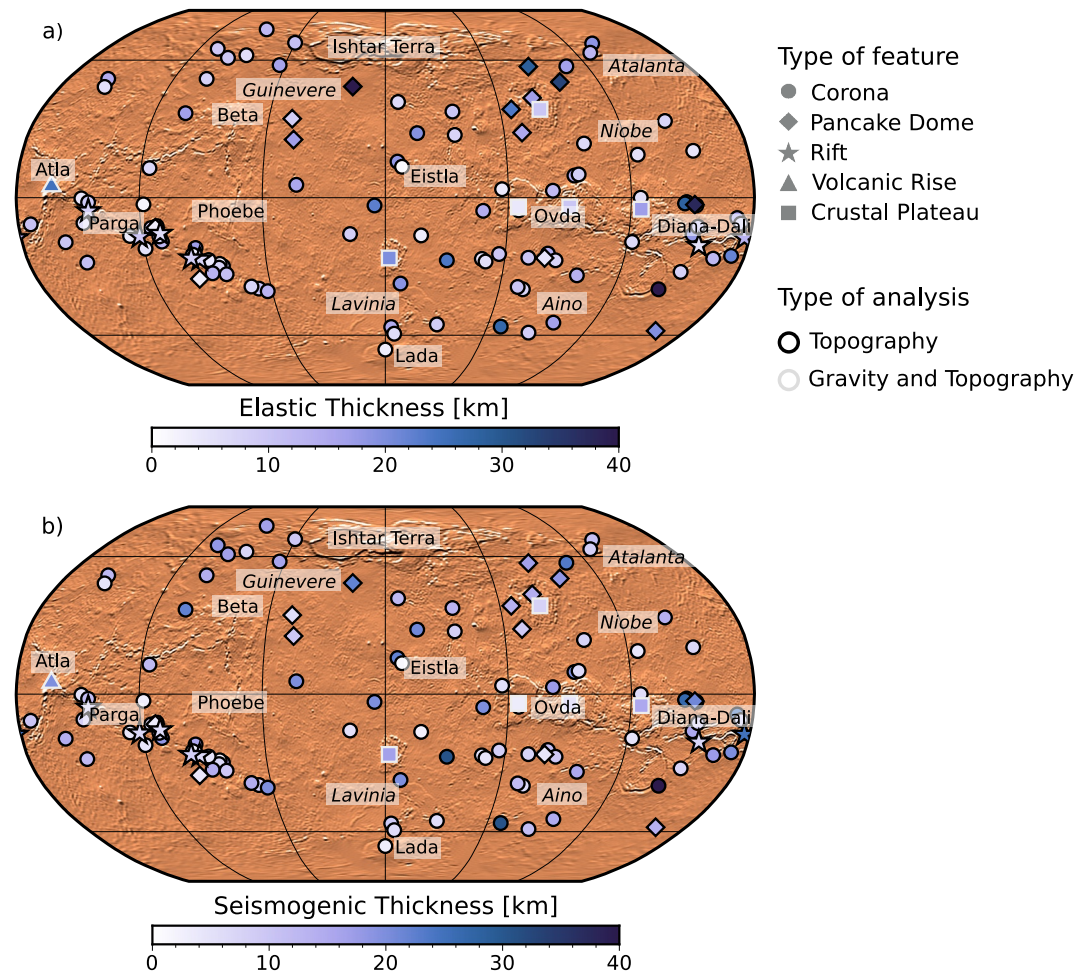


Figure 1. Global topography shaded relief maps of Venus showing (a) elastic thickness estimates from various studies (Borrelli et al., 2021; Maia & Wiczeorek, 2022; O'Rourke & Smrekar, 2018; Phillips et al., 1997; Smrekar et al., 2023) and (b) their corresponding seismogenic thickness based on the depth of the 600°C isotherm as a proxy. Our constraints from flexure suggest relatively thin seismogenic layers at the investigated features, with a median value of 9.7 km and a broad distribution ranging from 1 to 45 km. Symbol shapes indicate feature types, and symbol outlines indicate the type of analysis used to make the estimates (see text for details). Maps are in Robinson projection centered at 0° longitude. Labels specify major features on Venus, with normal font used for highlands and rift zones and italics for low-lying volcanic plains.

value for Venus estimates and a slow deforming region on Earth. This value is also typically used in Venus flexural studies (e.g., O'Rourke & Smrekar, 2018; Russell & Johnson, 2021; Smrekar et al., 2023). Figure 2b shows estimates using strain rate values of 10^{-17} s^{-1} and 10^{-15} s^{-1} , which correspond to an increase of 17% (11.8 km) and decrease of 14% (8.6 km) in the median seismogenic thickness, respectively.

The assumed rheology parameters for the viscous-deformation portion of the lithosphere also have important impact on our seismogenic thickness estimates. Our nominal model adopts a dry diabase rheology, commonly used for Venus' crust (Brown & Grimm, 1997; Mackwell et al., 1998; Maia & Wiczeorek, 2022; Phillips, 1994; Regorda et al., 2023). However, if the viscous lithosphere is primarily in the mantle, a dry olivine rheology is more appropriate. A composite model, incorporating a crustal layer over a mantle layer, would be more realistic but requires knowledge of crustal thickness. In general, such a scenario yields thermal gradient and seismogenic thickness estimates between those of pure diabase and olivine rheologies. In some cases, however, it may lead to two decoupled brittle zones (e.g., Ghail, 2015; Mackwell et al., 1998). Since a two-layer rheology depends on crustal thickness constraints—highly uncertain for Venus—and would introduce an additional free parameter, we chose not to explore this scenario. Instead, the pure dry diabase and dry olivine cases in Figure 2a can be interpreted as end-members representing a very thick and very thin crust, respectively. Adopting a dry olivine

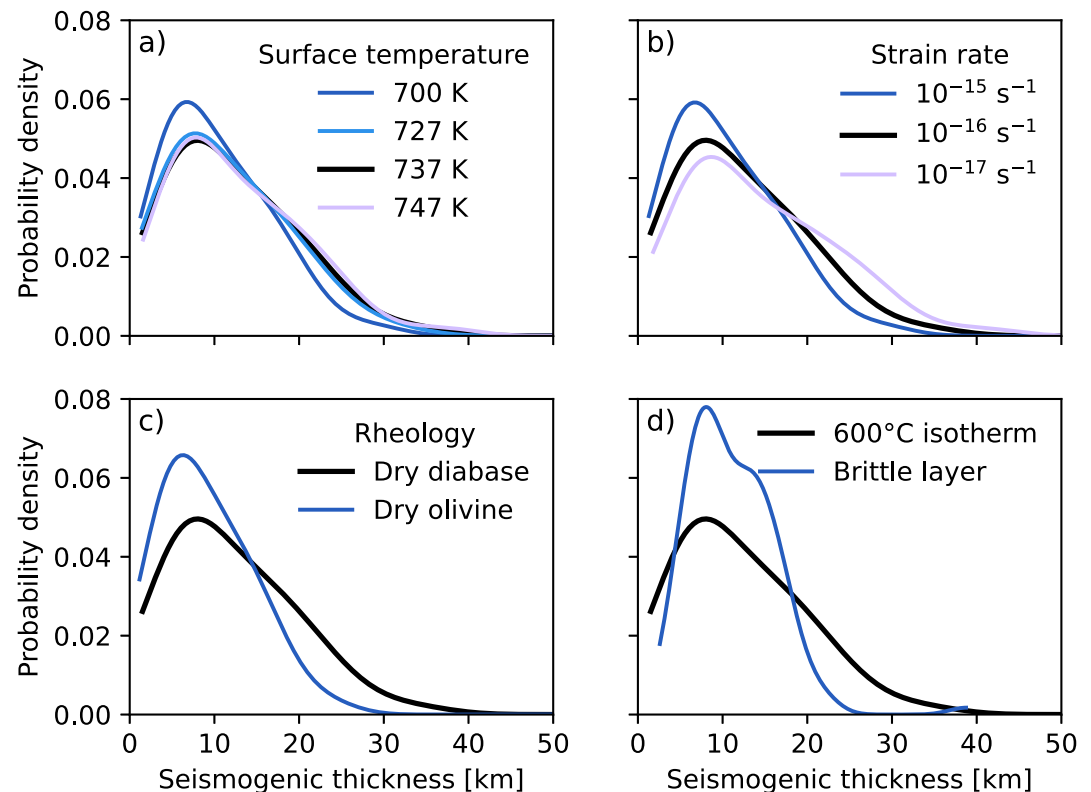


Figure 2. Sensitivity tests of seismogenic thickness based on lithospheric flexure analyses presented as the distribution of seismogenic thickness estimates. The reference results, shown in Figure 1b, are represented here by the black curves. Panels (a, b and c) show the impact of varying the lithosphere rheology, strain rate and surface temperature when computing the thermal gradient from the elastic thickness. Panel (d) presents the difference between computing the seismogenic thickness based on the 600°C isotherm and based on the transition depth between brittle and plastic deformation from the yield stress envelope. An analogous figure showing the effect of these parameters on the thermal gradient estimates can be found in Figure S3 of Supporting Information S1.

rheology, which is stronger than dry diabase, results in a median seismogenic thickness of 7.7 km (24% reduction compared to the diabase case). For the dry olivine rheology we use deformation parameters from Hirth and Kohlstedt (2004).

Figure 2d shows seismogenic thickness values defined as the transition depth between brittle to plastic deformation for extensional stresses, derived from the yield stress envelope. The estimates consider the same parameters as the reference case (i.e., diabase rheology, strain rate of 10^{-16} s^{-1} , and surface temperature of 737 K). Adopting the brittle-plastic transition instead of the 600°C isotherm as base of the seismogenic layer results in a narrower distribution, with minimum and maximum values of 2.5 and 39 km. On the other hand, the median barely changes, with a value of 10.2 km which correspond to a 1% increase. Although the depth of the brittle layer is a more accurate approximation of the seismogenic thickness (see Section 6.2 for a discussion), we focus the analysis on the 600°C isotherm to allow for a direct comparison between the different methods investigated in our study. Hence, the key finding of this comparison is that using the 600°C is a reasonable approximation to the actual depth of the brittle layer for intermediate seismogenic thickness values between ~5–20 km, but diverges at end-member estimates.

4. Seismogenic Thickness Estimates From Geodynamic Models

Next, we use geodynamic thermal evolution models employing parameters representative of the interior of Venus (Table S1 in Supporting Information S1) to estimate the possible range of seismogenic thickness at present-day. We employ the mantle convection code GAIA-v2 (Hüttig et al., 2013) in a 3D spherical geometry and model the thermal evolution of Venus over 4.5 Gyr. We include pressure- and temperature-dependent viscosity following an

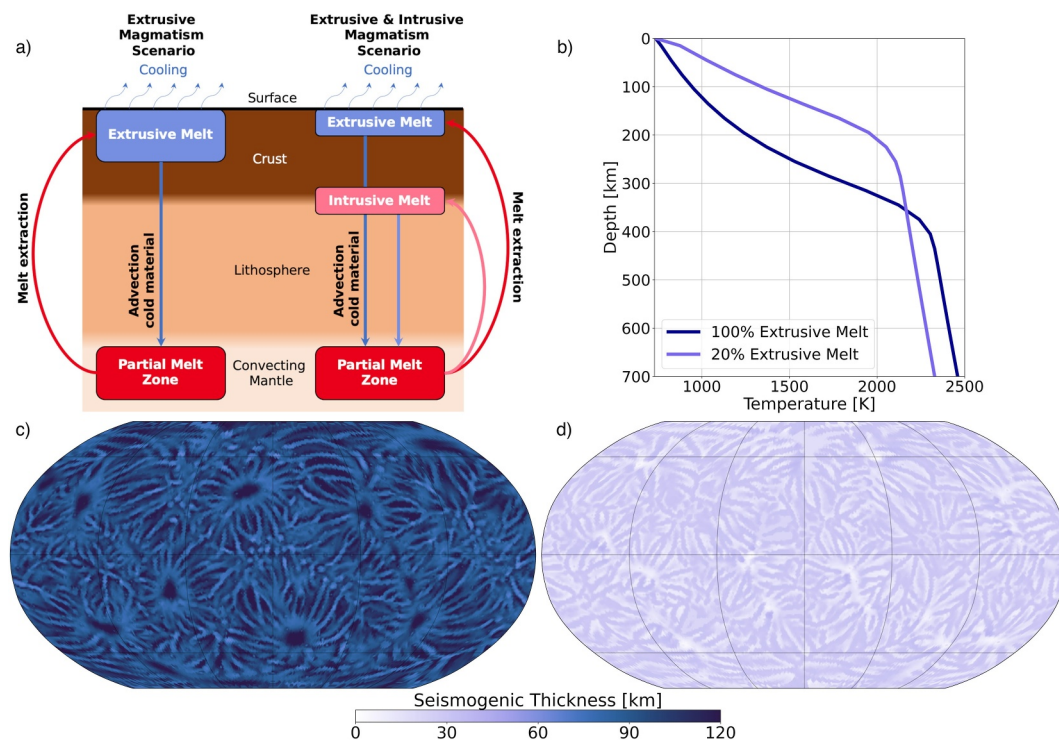


Figure 3. Seismogenic thickness estimates from geodynamic models. (a) Illustration of extrusive and intrusive magmatic heat transport in our models. (b) Laterally averaged thermal profiles after 4.5 billion years of thermal evolution in the uppermost 700 km for a fully extrusive model and a hybrid extrusive-intrusive model of Venus. (c) Distribution of the seismogenic thickness in the fully extrusive model. (d) Distribution of the seismogenic thickness in the hybrid extrusive-intrusive model, that is, assuming that 80% of the produced melt volume remains trapped in the subsurface at 45 km depth. Including intrusive melt processes yields a significantly lower seismogenic thickness than a fully extrusive model, aligning more closely with constraints from flexural analysis. The effect of magmatic intrusions on the seismogenic thickness is shown in Figure 4 for different intrusion depths and extrusive fractions.

Arrhenius law, as well as thermal conductivity and expansivity following the parametrization of Tosi et al. (2013). In addition, we account for core cooling and the decay of radioactive heat sources. The models consider partial melting of the mantle using the method presented in Padovan et al. (2017), adopting the solidus and liquidus parameterization of Stixrude et al. (2009) derived for the mantle of the Earth. The details of the code and model setup can be found in the, Section S1 of Supporting Information S1.

Our models consider intrusive and extrusive magmatism (Lourenço & Rozel, 2023; Rolf et al., 2022; Tian et al., 2023). The effects of the magmatic style on the heat transport through the lithosphere and crust are schematically illustrated in Figure 3a. While extrusive magmatism efficiently cools and thickens the lithosphere through the downward advection of cold surface material beneath newly extruded melt, magmatic intrusions heat the shallow subsurface and may lead to lithospheric delamination and foundering (see Figure S2 in Supporting Information S1). On Venus, the ratio of extrusive to intrusive melt is poorly known. On Earth, compilations of time-averaged volumetric rates of volcanic output and magma emplacement indicate that only 20% of the melt volume reaches the surface in oceanic regions, and as little as 10% in continental areas (Crisp, 1984). Assuming most of Venus' surface is basaltic and similar to oceanic crust on Earth (Surkov et al., 1984, 1986), we choose an extrusive fraction of 20%.

Figure 3b shows the upper mantle temperature profiles for models in which 80% of the melt remains trapped in the lithosphere at 45 km depth versus entirely extrusive magmatism. While fully extrusive magmatism was typically used in early global geodynamic models of Venus (Armann & Tackley, 2012; Nakagawa & Tackley, 2012; Ogawa & Yanagisawa, 2011), more recent studies acknowledge the importance of intrusive magmatism for the global geodynamic and tectonic regime of Venus (Lourenço et al., 2020; Rolf et al., 2022; Tian et al., 2023). We estimate the range of seismogenic layer thicknesses for these models using the 600°C isotherm as a proxy.

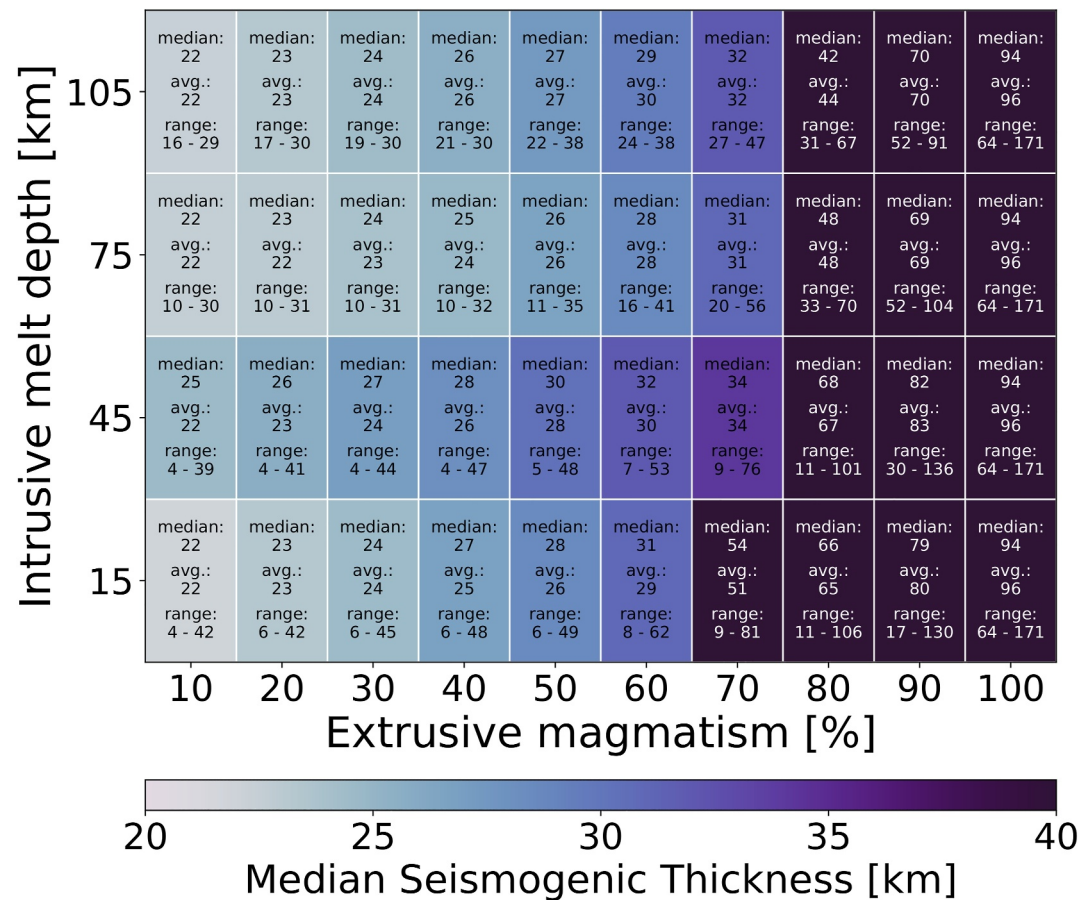


Figure 4. Summary of seismogenic thickness estimates obtained from geodynamic thermal evolution models using various extrusive fractions and the emplacement depth of intrusive melt using the 600°C isotherm as a proxy. Each cell in the heat maps represents a global 3-D geodynamic thermal evolution model. The seismogenic thickness estimates inside the cells are in kilometers. Similar summary plots considering the 500°C and 800°C isotherms as proxies for the seismogenic thickness are shown in the Figure S5 of Supporting Information S1. A discussion on the choice of the cut-off isotherm is presented in Section 6.2.

In the fully extrusive geodynamic model, efficient melt extraction results in a thick and cold lithosphere (Figure 3b), a behavior reported also by other geodynamic studies (Lourenço et al., 2018; Moore & Webb, 2013). This thick and cold lithosphere leads to a small thermal gradient and a thick seismogenic layer ranging between 64 and 171 km (Figure 3c). We particularly observe a thick seismogenic layer at the locations of mantle plumes (i.e., at regions where partial melt, and thus heat, is removed from the interior and extracted to the surface, cf. Figure 3c, where the plume heads are located below the roughly circular areas of thick seismogenic lithosphere). In contrast, the model with a large fraction of intrusive melt (80%) results in a warmer lithosphere and hence lower seismogenic thickness, ranging between 4 and 41 km (Figure 3d). Areas with the thinnest seismogenic layer are characterized by the presence of hot magmatic intrusions in the subsurface. The largest differences in the average mantle temperatures between these two models occur in the lithosphere (i.e., between 50 and 300 km depth), with differences as high as 714 K at 195 km depth (Figure 3b).

Figure 4 summarizes the effect of varying the intrusive-to-extrusive ratio and the emplacement depth of intrusive magmatism on the seismogenic thickness. The seismogenic thickness estimates are mainly controlled by the ratio of intrusive to extrusive magmatism. Nevertheless, for models with a predominance of intrusive melts (over 50% intrusions), the seismogenic thickness is only mildly affected. For example, for an intrusive melt emplacement depth of 45 km the median seismogenic thickness increases approximately linearly from 25 to 30 km up to 50% extrusive magmatism, but jumps to a median value of 68 km for 80% of extrusions. In comparison, the melt depth

has a minor influence. In the case of 20% extrusion the melt depth changes the median seismogenic thickness by 3 km at most.

5. Seismogenic Thickness Estimates From Mantle Density Anomalies

Venus' long-wavelength (>1,000 km) gravity and topography signatures are predominantly driven by convective flows in the mantle (e.g., Herrick & Phillips, 1992; Kiefer et al., 1986; Phillips et al., 1981). Several studies of topography and gravity have used viscous flow models (e.g., M. A. Richards & Hager, 1984) to investigate the geophysical properties of Venus' mantle, enabling them to determine the distribution of density anomalies in the mantle (James et al., 2013; Maia et al., 2023; Pauer et al., 2006; Steinberger et al., 2010). These studies indicate that large volcanic rises, such as Atla and Beta Regiones, are associated with low-density anomalies, while low-lying plains are associated with relatively high-density anomalies in the mantle. A likely source for these lateral density variations is the presence of temperature anomalies due to mantle convection. These anomalies cause temperature variations at the base of the thermal lithosphere which, in turn, affect the lithospheric thermal gradient and the seismogenic thickness.

Here, we estimate Venus' seismogenic thickness associated with mantle temperature anomalies inferred from dynamic gravity-topography investigations. We compute temperature anomalies using the map of mantle density anomalies at 250 km depth from Maia et al. (2023) since it is publicly available and in line with previous studies (e.g., James et al., 2013). We focus on the so-called “nominal scenario” in Maia et al. (2023), where density anomalies are parameterized as a thin mass-sheet. In this approximation, density anomalies are, by definition, in kg/m^3 . This approach is commonly considered a good representation of mantle plume heads (e.g., Herrick & Phillips, 1992; James et al., 2013), typically distributed within a relatively thin layer below the lithosphere (e.g., French & Romanowicz, 2015; Sleep, 1990; Smrekar et al., 1997). To convert the mass-sheet to volumetric density anomalies, a layer thickness d_p must be specified (here defined as 300 km). Hence, from the density anomaly distribution $\Delta\rho$, the mantle temperature anomalies ΔT can be estimated as:

$$\Delta T(\theta, \phi) = \Delta\rho(\theta, \phi) d_p^{-1} \alpha^{-1} \rho_0^{-1}, \quad (2)$$

where α is the thermal expansivity, and ρ_0 is the reference mantle density in the uppermost mantle, set to $3 \times 10^{-5} \text{ K}^{-1}$ and $3,300 \text{ kg/m}^3$, respectively, based on representative values from Earth mantle rocks (e.g., Turcotte & Schubert, 2002). Latitude and longitude are denoted by θ and ϕ , respectively. Moreover, we define that the volumetric density anomalies have a fixed layer thickness of $d_p = 300 \text{ km}$. We chose this value because it overall leads to temperature anomalies with magnitudes similar to hotspots on Earth (e.g., Bao et al., 2022; Putirka, 2008; Schilling, 1991; White & McKenzie, 1995). Note that this approach assumes that the density variations are entirely caused by temperature anomalies, even though composition can also play a role. Hence, our estimates are an upper limit for the temperature anomalies for a given parameter set.

Since these constraints are only sensitive to lateral temperature variations, a final assumption required to constrain the seismogenic thickness is the average mantle temperature at the base of the lithosphere. For this, we choose to use the average temperature profile from the 80% intrusive geodynamic model (Figure 3b), as this model aligns best with the lithospheric thermal gradients derived from the elastic thickness constraints (see Section 6, for discussions). The highly intrusive scenario has a corresponding lid thickness (i.e., the thermal lithosphere where velocities are close to zero) of about 100 km, hence we pick the temperature at this depth as the average temperature at the base of the lithosphere, which corresponds to 1,370 K. A thermal lithosphere thickness of 100 km is also supported by gravity and topography investigations (Maia et al., 2023; Pauer et al., 2006). We then estimate the thermal gradient and derived seismogenic thickness (Equation 1) using this average temperature and the temperature variations as defined in Equation 2.

Notwithstanding the required assumptions, our approach provides a global view of the spatial distribution of temperature anomalies in the mantle and the associated lateral variations in seismogenic thickness (Figure 5). Volcanic rises such as Eistla, Lada, Phoebe, and Imdr are associated with temperature excesses at 100 km depth in the range of 100–250 K. The largest temperature excesses are associated with the volcanic rises Atla and Beta, reaching over 300 K, which also correspond to the thinnest seismogenic layer, with a minimum of 11 km. In contrast, the low-temperature anomalies and the regions with the thickest seismogenic layer are the low-lying volcanic plains. In particular, the Atalanta Planitia is associated with the thickest seismogenic layer (over

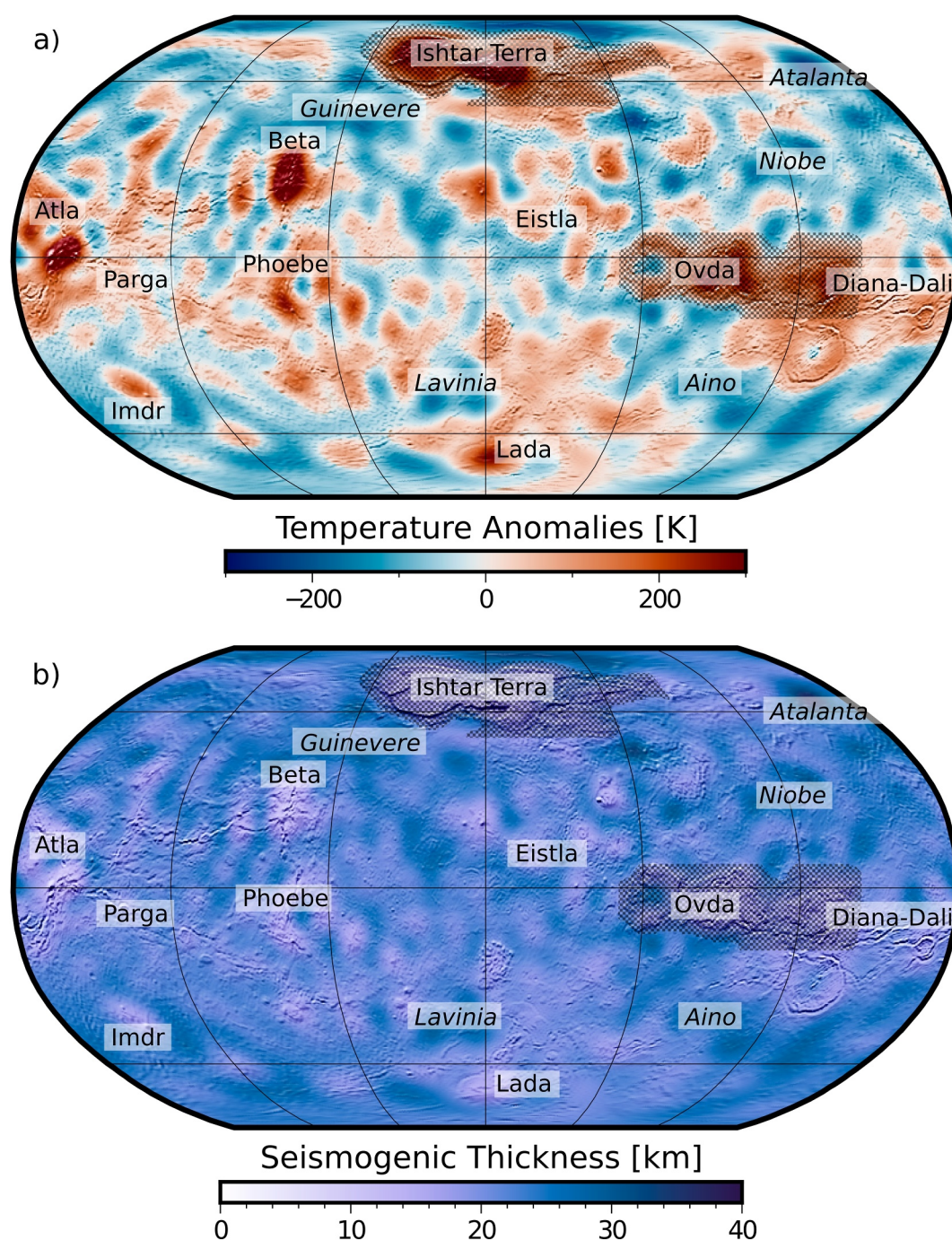


Figure 5. Global distribution of (a) temperature anomalies in the upper mantle and (b) the seismogenic thickness of Venus based on the density anomaly constraints obtained by Maia et al. (2023). These estimates indicate that volcanic rises, commonly associated with deep-seated “hotspot” plumes (e.g., Stofan et al., 1995), have relatively thin seismogenic layers, whereas volcanic plains are associated with thicker seismogenic layers. Both maps are in Robinson projection centered at 0° longitude and are overlain by a shaded relief map. Hatched regions (Onda Regio, Thetis Regio, and Ishtar Terra) should be ignored as they were excluded from the localized spectral analysis used to constrain the density anomalies. Labels specify major features on Venus, with normal font indicating highlands and rift zones, and italics indicating low-lying volcanic plains.

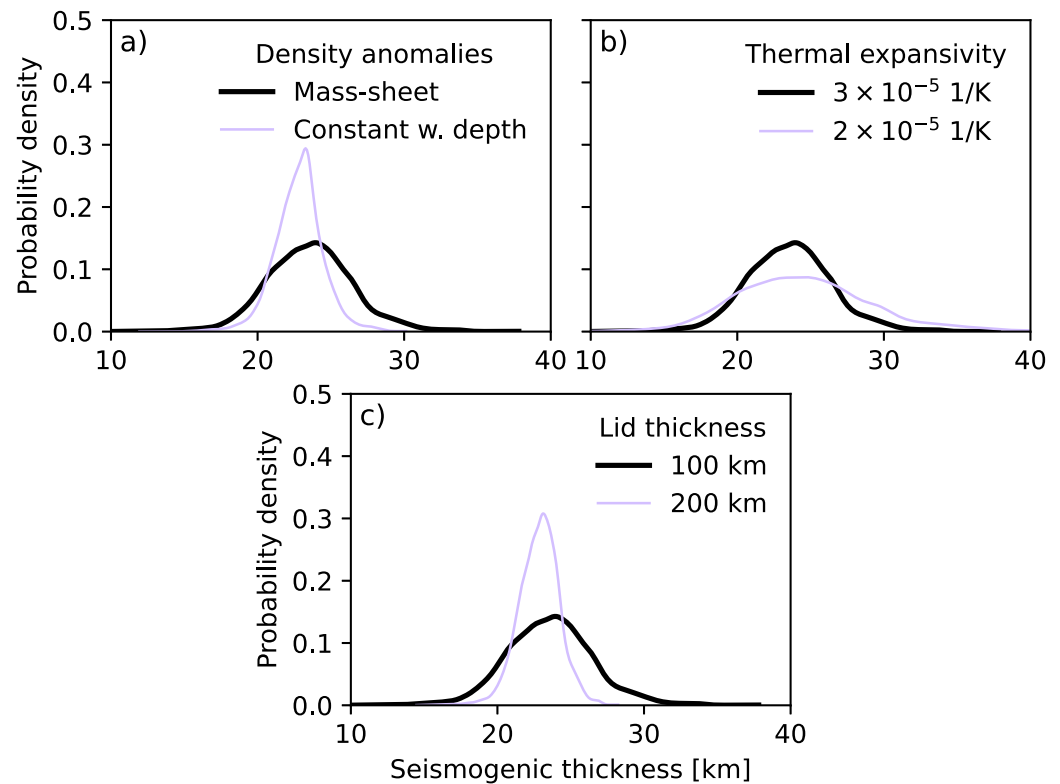


Figure 6. Sensitivity tests of seismogenic thickness estimates based on constraints for mantle density anomalies. The black curves correspond to the estimates of the reference distribution shown in Figure 5b. Panel (a) presents the effect of the parametrization approach used to estimate the distribution of mantle density anomalies, either modeled as a thin layer at a specific depth within the mantle or assumed to be constant with depth throughout the mantle, as investigated in Maia et al. (2023). Panel (b) shows the impact of thermal expansivity used in the conversion from density anomalies to thermal anomalies (Equation 2), and panel (c) displays the effect of varying the lid thickness, which corresponds to the depth where the heat generated in the deep interior is transported only by heat conduction. An analogous figure showing the effect of these parameters on the thermal gradient estimates can be found in the Figure S4 in Supporting Information S1.

35 km). Finally, we note that the hatched regions in Figure 5 (Ishtar Terra, Ovda Regio and Thetis Regio) were originally excluded from the geophysical inversion performed in Maia et al. (2023) since they are known to be dominated by shallow support mechanisms and not dynamic compensation. Therefore, these are disregarded in this analysis.

Sensitivity tests of input parameters are presented in Figure 6, showing the effects of the choice of parameterization of (a) mantle density anomalies (see Maia et al., 2023, for details), (b) thermal expansivity, and (c) lid thickness. When assuming that the density anomalies have a constant distribution throughout the mantle, the pattern of anomalies is very similar to the thin mass-sheet case but their amplitudes are smaller, since they are not concentrated in a single thin layer. This scenario leads to a narrower distribution of seismogenic thickness estimates (Figure 6a), associated with a 43% decrease in standard deviation (from 3 to 1.7 km). The thermal expansivity also has a significant impact on the seismogenic thickness estimates, since the calculation of temperature from density anomalies is inversely proportional to this parameter. Yet, its value for Venus mantle is not well constrained, with many studies assuming $2 \cdot 10^{-5}$ or $3 \cdot 10^{-5} \text{ K}^{-1}$ (Gülcher et al., 2023; James et al., 2013; Regorda et al., 2023; Rolf et al., 2018; Uppalapati et al., 2020). Figure 6b shows that decreasing the thermal expansivity from $3 \times 10^{-5} \text{ K}^{-1}$ to $2 \times 10^{-5} \text{ K}^{-1}$ leads to a larger range of seismogenic thicknesses, with standard deviation increasing 66%, from 3 to 5 km. Lastly, the value assumed for the average thermal lithosphere thickness impacts the lithospheric thermal gradient and, consequently, the seismogenic thickness. By increasing the lithosphere thickness to 200 km (while keeping the same average temperature of 1,370 K at the base of the lithosphere) the standard deviation of the distribution of seismogenic thickness estimates decreases to 1.4 km. Although all the investigated parameters have a significant effect in the standard deviation (or width) of the distribution, they have a negligible impact on the median value, with shifts of less than 1 km in all tested cases.

6. Discussion

6.1. Combined Interpretation of Different Seismogenic Thickness Estimates

A summary comparing the results from the three different approaches is given in Figure 7. The left panels show estimates from local flexural analyses considering a lithospheric dry diabase rheology and a strain rate of 10^{-16} s^{-1} (as in Figure 1), and a scenario assuming a dry olivine (stronger) rheology and a higher strain rate of 10^{-15} s^{-1} . Changing the rheology from dry diabase to dry olivine and decreasing the strain rate do not significantly affect the results; they shift the seismogenic thickness to slightly lower values, with the mean dropping from 12 to 8 km. The center panels show the geodynamic model estimates for the fully extrusive magmatism and the 80% intrusive magmatism cases (see maps in Figure 3). The magmatic style significantly impacts the lithospheric thermal structure and seismogenic thickness. The fully extrusive volcanism case has a cold lithosphere and hence thick seismogenic layer that is never less than 50 km thick. The right panels present estimates from mantle density anomaly constraints, with two cases using distinct sets of parameters that lead to the maximum and minimum variance of the distribution of the estimated seismogenic thickness, both taking the reference temperature profile from the 80% intrusive magmatism model (as in Figure 5). We show estimates using the density anomalies from the thin mass-sheet scenario placed at 250 km depth, assuming a lithosphere thickness of 100 km and a thermal expansivity of $2 \times 10^{-5} \text{ K}^{-1}$. The other estimates consider uniformly distributed density anomalies from the base of the lithosphere to the core-mantle boundary (resulting in smaller amplitude anomalies), assuming a lithosphere thickness of 200 km and a thermal expansivity of $3 \times 10^{-5} \text{ K}^{-1}$. These estimates show that the contribution to the seismogenic thickness from temperature variations in the mantle can range from less than 10 to several tens of kilometers, depending on the parameters considered. In reality, the contribution from these mantle structures probably lies somewhere in between these two cases.

Comparing the estimates from flexural analysis and the 80% intrusive magmatism geodynamic model, the distributions of seismogenic thickness values overlap significantly, but elastic thickness estimates skew towards lower seismogenic thicknesses. This is likely because many of the features investigated by flexural studies, such as coronae and rifts, are likely associated with magmatic processes that present locally high thermal gradients. Indeed, high thermal gradients within geodynamic models are associated with regions of small-scale melt intrusions in the lithosphere. Meanwhile, estimates from mantle density anomalies never reach such high thermal gradients. This indicates that not only can mantle plumes regionally decrease the seismogenic thickness via increased heat conduction through the lithosphere, but also that intrusions play an important role in heating the lithosphere and decreasing the seismogenic thickness on a local scale.

We find that, under the 600°C isotherm approximation, the seismogenic thickness of Venus globally varies from 2 to 35 km (shown by the orange area in Figure 7b). This range is defined by the 1st and 99th percentiles of the combined distribution of all estimates, excluding the extrusive model. The combined median seismogenic thickness is 22 km, while the thermal gradient has a median value of 7 K/km. For the combined analysis, each approach considered is given the same weight. Since the average crustal thickness of Venus is estimated to be between 10 and 25 km (James et al., 2013; Maia & Wiczeorek, 2022; Simons et al., 1997), it is probable that in many places the seismogenic layer encompasses the entire crust and a few kilometers of the lithospheric mantle. This scenario is more likely in regions of thin crust and cold lithospheres, such as volcanic plains. On the other hand, in highlands associated with thick crust, such as the crustal plateaus and Ishtar Terra, the seismogenic layer could be thinner than the crust itself. The same is true for regions of anomalously high thermal gradients where the seismogenic thickness is typically lower than 10 km, as is the case for many coronae and rift zones investigated by flexural analysis.

The outlier point in the flexural analysis corresponds to the measurement taken at the southeastern rim of Artemis corona (132.1°E longitude and 32.5°S latitude), an exceptionally large volcano-tectonic feature about 2,500 km in diameter. This discrepancy suggests that the simple flexure models used for elastic thickness estimates inadequately explain the complexity of this region. Suggestions of active regional-scale subduction at the southeastern arc of Artemis (Davaille et al., 2017; Gülcher et al., 2020; McKenzie et al., 1992; Sandwell & Schubert, 1992) indicate that in-plane forces may strongly impact the flexure profile in this region (Mueller & Phillips, 1995). A relatively strong lithosphere at the margin of Artemis is expected, however, as a combination of a strong lithosphere (cold lithosphere; thin crust) and a buoyant mantle plume is necessary to promote the proposed subduction-like response at a plume margin on Venus (Davaille et al., 2017; Gülcher et al., 2020, 2023). The largest seismogenic thickness values obtained from density anomalies estimates are at Atalanta planitia, a volcanic plain

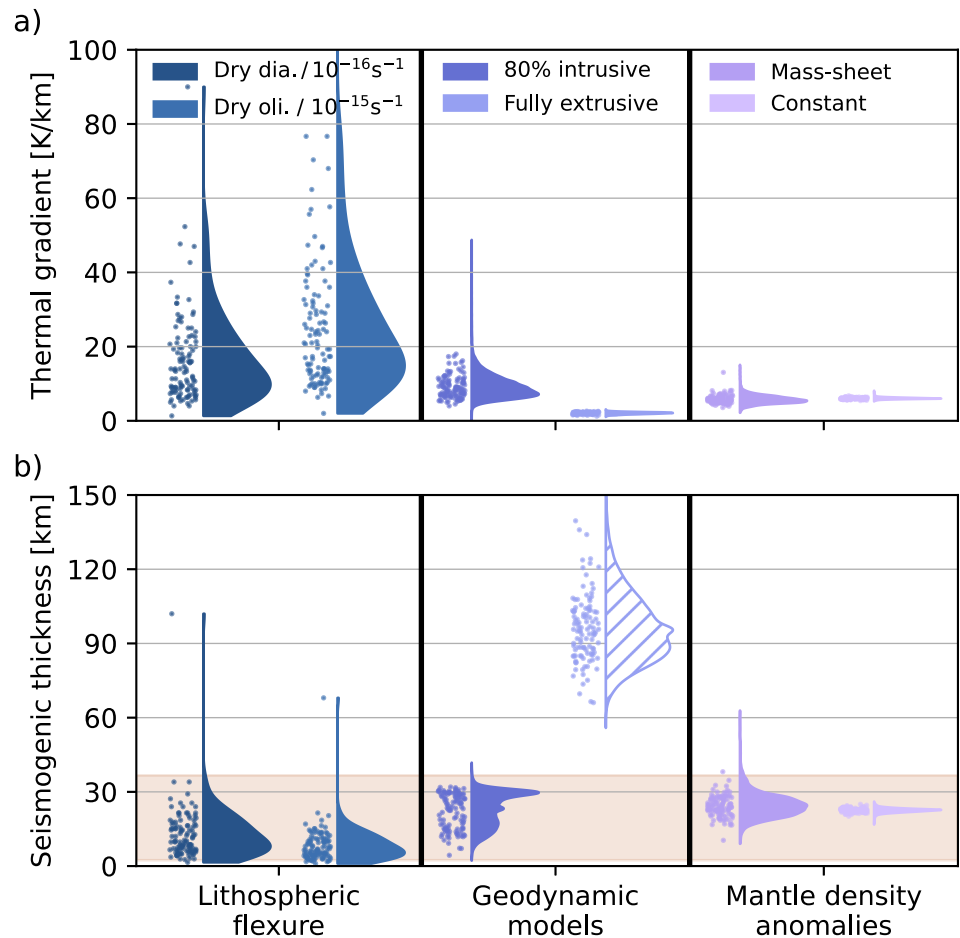


Figure 7. Distributions of (a) thermal gradient and (b) seismogenic thickness estimates using the different methods explored in this study. Each set of estimates is presented both as a scatter plot and a kernel density distribution with the range of values on the y-axis. The left panels show estimates based on regional flexure studies (Section 3). The center panels present estimates based on thermal evolution models with distinct magmatic styles (Section 4). The right panels show estimates from mantle density anomalies using geophysical inversions of gravity and topography data (Section 5). Our results show that the fully extrusive case (hatched fill) is inconsistent with the observational constraints. Considering all other estimates, we find that the seismogenic thickness ranges from 2 to 35 km, based on the 1st and 99th percentiles of the combined distribution. This range is indicated by the orange area in panel (b). Note that these constraints take 600°C as a threshold for the seismogenic thickness. A similar plot showing estimates considering 500°C and 800°C are available in the, Figure S6 of Supporting Information S1.

extending from approximately 120°E to 180°E longitude and 50°N to 75°N latitude, where the density anomalies obtained by Maia et al. (2023) are largest. The volcanic plains, such as Atalanta, are commonly interpreted as regions of mantle downwellings (e.g., James et al., 2013; Maia et al., 2023).

Finally, we note that these results are in agreement with the first-order estimates from Van Zelst et al. (2024), but support a larger range of values since we include different independent analyses and test a larger variety of parameters when computing the seismogenic thickness. More importantly, we are able to map in which regions we expect the seismogenic thickness to be thinner or thicker, while they only provide a uniform range for the entire planet. On the other hand, these estimates are still bounded by the assumption that the seismogenic thickness is defined as the depth of the 600°C isotherm which may not be necessarily true (see Section 6.2 for a discussion).

6.2. Temperature-Dependence of Seismogenic Thickness: From Observations to Laboratory Experiments

Throughout this study, we estimated the seismogenic thickness based on the assumption that it corresponds to the 600°C isotherm. This value is typically taken as a reference value for the Earth, particularly for Earth's oceanic

lithosphere (Jackson et al., 2008; McKenzie et al., 2005), while continental regions with strong (probably dry and mafic) rheologies experience quakes down to the base of the crust (~35 km) where temperatures can reach between 500 and 600°C (Déverchère et al., 2001). Nevertheless, most continental earthquakes nucleate within the upper crust, at depths shallower than 20 km and temperatures colder than 350°C (e.g., Chen & Molnar, 1983). This discrepancy shows that temperature alone does not define the thickness of the seismogenic layer, and other properties also play important roles. The rock composition is one key factor: felsic and hydrous rocks are weaker than mafic and dry rocks (e.g., Mackwell et al., 1998). Moreover, highly dynamic geological and tectonic conditions can lead to thicker (and hotter) seismogenic layers. For example, earthquake depth constraints at the Iceland hotspot indicate depth limits of the seismogenic layer corresponding to temperatures of $750 \pm 100^\circ\text{C}$ (Ágústsson & Flóvenz, 2005). Additionally, tectonically active regions on Earth associated with high strain rates (10^{-16} – 10^{-13} s^{-1}) can produce earthquakes at higher temperatures, in the range of 700–900°C (Molnar, 2020).

Beyond seismological investigations, laboratory experiments are fundamental tools to understand the rheological properties of planetary crusts and mantles and investigate how Venus' seismic potential may differ from Earth's. As described in Scholz (1998), the onset of quakes is driven by fault instability and the transition from unstable to stable faulting at depth typically coincides with the change in deformation behavior from brittle to plastic. In fact, the depth of the brittle-plastic transition classically defines the maximum seismogenic thickness (e.g., Scholz, 1998). Although temperature is a key factor, laboratory studies show that other parameters, such as pressure, composition, and the presence of glass, strongly influence the onset of brittle deformation. Edmond and Paterson (1972); Tullis and Yund (1977) demonstrated that brittle behavior is favored under lower pressures, a factor particularly relevant for Venus, where the same temperatures are reached at shallower depths (and thus lower pressures) than on Earth. Rock composition is also critical. Mafic rocks typically exhibit more brittle behavior than felsic ones (e.g., Scholz, 1998), in agreement with the seismic observations. Moreover, the presence of glass reduces rock strength considerably Violay et al. (2012). Another important finding from experiments is that the brittle-to-plastic transition is characterized by a gradual change, defined as a transitional field where both brittle and plastic deformation can happen (Hirth & Tullis, 1994; Kohlstedt et al., 1995; Scholz, 1998). For quartz, the brittle to semi-brittle transition occurs at 300–400°C (e.g., Tullis & Yund, 1977); for feldspar, estimates range from 450 to 650°C (Tullis & Yund, 1977; Voll, 1976); and for olivine, around 600°C (Boettcher et al., 2007). For polyphase aggregates like basalts, Violay et al. (2012) showed that non-glassy basalts, potentially analogous to Venus' crust, can remain brittle up to $550 \pm 100^\circ\text{C}$.

Thus, although temperature is a valuable proxy, a single isotherm cannot precisely capture the extent of the brittle zone of a planet. The true thickness of the seismogenic layer also depends on rock properties and deformation mechanisms. In addition, the existence of a semi-brittle field adds more complexity when defining the portion of the planet where rocks can rupture and quakes can take place. Quakes can propagate into the semi-brittle field below the brittle zone, extending the region of seismic energy release deeper than the nucleation depth (e.g., Scholz, 1998). These entangled concepts are illustrated in Figure 8. This figure distinguishes between the temperature-defined seismogenic thickness used in our study, the “true” brittle–plastic boundary, the earthquake nucleation zone, and the deeper rupture propagation zone. The nucleation zone, marked in red in Figure 8, starts a few kilometers below the surface which can be explained by the presence of unconsolidated and/or clay-rich fault gouge (Scholz, 1998) and goes down to the base of the brittle layer. It is also important to remark that the yield stress envelope shown in Figure 8 is a simplified model that considers a single type of rock which results in a single brittle layer. Yet, it is possible that, at least in some regions, Venus' mechanical lithosphere has two distinct brittle layers, the upper one of which is associated with upper crustal rocks and the lower one with upper mantle rocks (see Section 3 for details).

So, is the 600°C isotherm a valid proxy for estimating seismogenic thickness on Venus? Of course, the use of a single isotherm is a simplification. On Earth, the relevant temperature for seismicity varies depending on lithospheric type, rock composition, tectonic history, and strain rate (e.g., Albaric et al., 2009; Craig & Jackson, 2021; Déverchère et al., 2001; Jackson et al., 2008). It is also important to keep in mind that an Earth-to-Venus analogy is never perfect. For example, the thickness of Venus' crust is probably in between continental and oceanic crust on Earth, approximately 20 km on average (e.g., Maia & Wiczorek, 2022); the pressures on Venus are lower for the same temperature range; and Venus' lithosphere is probably drier. Nevertheless, the 600°C has been shown to be a good reference value for the Earth, being associated with the quake temperature threshold for the mantle within the oceanic lithosphere and for the lower crust of continental regions with strong rheology. All in all, since different studies have shown that Venus' crust likely has a dry and strong rheology (Foster & Nimmo, 1996;

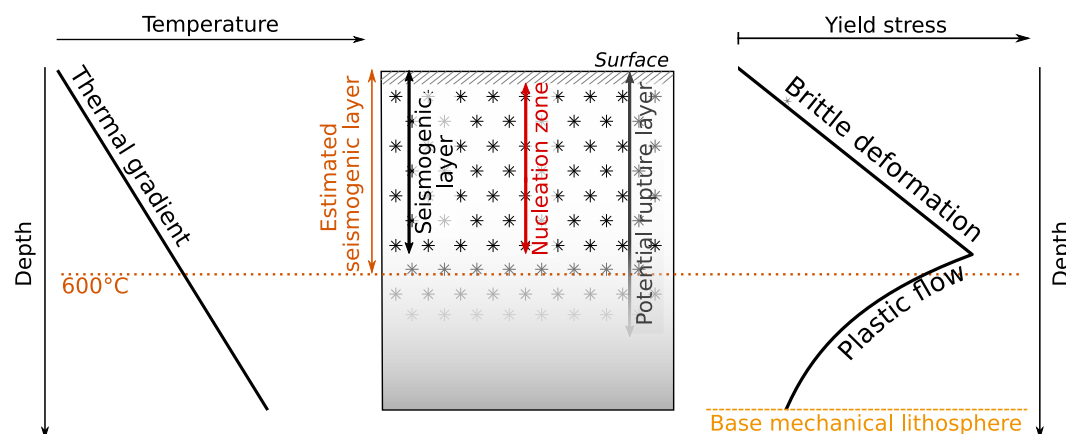


Figure 8. Schematic view of the nomenclature surrounding seismogenic thickness. The left panel illustrates a lithospheric thermal gradient, assumed linear throughout this study, and the associated depth of the 600°C isotherm. The central panel shows different layer definitions associated with seismogenesis. The estimated seismogenic layer represents the portion of the lithosphere with temperatures lower than 600°C, used in our analyses as a proxy for the seismogenic layer. The “true” seismogenic layer extends from the surface down to the boundary between brittle and plastic deformation, while the nucleation zone starts a few kilometers below the surface extending down to the brittle plastic transition. On Earth, quakes typically do not nucleate at shallow depths (less than ~2 km) due to the predominance of unconsolidated materials near the surface (e.g., Scholz, 1988). Observational constraints have shown that quakes can propagate beyond the brittle-plastic transition into the so-called semi-brittle field (e.g., Déverchère et al., 2001). Hence the area of potential rupture propagation extends deeper into the lithosphere than the nucleation zone. The right panel shows a simplified rheological model of the mechanical lithosphere for extensional stress. The transition from brittle to plastic deformation corresponds to the base of the seismogenic layer. Note that we consider here a simple model of lithospheric strength with only one composition and assuming a sharp boundary between brittle and plastic regimes, neglecting the semi-brittle field.

Kaula, 1990; Kohlstedt & Mackwell, 2009; Nimmo & Mackwell, 2023; Regorda et al., 2023), we find it reasonable to assume that the 600°C isotherm is a fair approximation for Venus' seismogenic layer globally.

In contrast, Karato and Barbot (2018) argued that Venus should be aseismic. Their study assumed seismic thresholds of 400°C for the crust and 600°C for the mantle, combined with a 30 km-thick crust, resulting in a lithospheric structure too hot for quake nucleation. However, we consider this scenario unlikely for two main reasons. First, laboratory experiments on basaltic rocks indicate that brittle behavior is possible well above surface temperatures (Tullis & Yund, 1977; Violay et al., 2012). Second, the assumed crustal thickness is high: global estimates range from 10 to 25 km, with 30 km or more typically related to regions of thickened crust, such as Ishtar Terra and crustal plateaus (James et al., 2013; Maia & Wiczorek, 2022). Thus, even when considering that the crust is too hot for brittle failure, seismicity could still occur in the mantle. It is true, however, that this would imply a much more modest level of seismicity.

Hence, to account for the uncertainties in deformation temperature thresholds, we explore a range of plausible scenarios. Considering the findings of rock deformation studies for basalts and feldspar (Tullis & Yund, 1977; Violay et al., 2012; Voll, 1976) we adopt a maximum temperature of 500°C as lower bound, yielding seismogenic thicknesses of 0.5–10 km. As an upper bound, we use 800°C which is commonly used as an upper limit for seismicity in extreme geological environments (Ágústsson & Flóvenz, 2005; Molnar, 2020). This leads to seismogenic thickness values of 5.8–92 km. More details on these constraints can be found in the, Figure S6 of Supporting Information S1. Based on all the estimates presented here, taking into account the scenario proposed by Karato and Barbot (2018), and adopting a reference average crustal thickness value of 20 km (e.g., Maia & Wiczorek, 2022), we establish three different scenarios for Venus' seismogenic layer:

1. A single, thick seismogenic layer. When taking 600°C or higher temperatures as a proxy for the depth of the seismogenic layer, it generally encompasses the entire crust and the uppermost mantle. In regions associated with hotspots and considerable magmatic activity the seismogenic thickness is locally reduced and does not reach the mantle. The difference between taking the 600°C and 800°C isotherms as a proxy translates into how much of the mantle is potentially seismogenic. For 600°C, this means the uppermost ~5–15 km, while for 800°C the seismogenic layer reaches 20–50 km into the mantle.

2. Decoupled seismogenic layers. In a scenario where the crust can be seismogenic up to 500°C and the mantle up to 600°C, Venus would have one thin seismogenic layer in the upper crust (up to 10 km depth), an aseismic lower crust, and a second seismogenic layer in the uppermost mantle with a thickness of about 5–15 km.
3. Mantle-only seismogenic layer. If the Venusian crust behaves seismically only for temperatures below the planet's surface temperature as suggested by Karato and Barbot (2018), only the uppermost mantle could be subjected to quake nucleation. In this case the seismic potential of Venus would be strongly limited. Taking into account experimental and observational constraints from basaltic rocks (e.g., Violay et al., 2012), we consider this scenario unlikely.

6.3. Implications for Seismicity on Venus

It is important to note that the three different scenarios for Venus' seismogenic layer—and the resulting thickness range of 2–35 km—address only the planet's lithosphere seismogenic potential; they do not necessarily translate to seismicity depths on Venus. In other words, while the presence of a seismogenic layer is a requirement for any kind of seismicity to occur on a planet, it does not mean that seismicity will occur if there is a seismogenic layer. Indeed, the Earth has a global seismogenic layer in both continental and oceanic lithosphere, yet earthquakes are largely confined to plate boundaries, leaving vast regions with seismogenic potential effectively aseismic. The reason for this is that potential seismicity is not directly defined by the seismogenic zone or indeed brittle behavior. Instead, whether slip localizes as an earthquake or is released aseismically depends on many factors, such as the local stress field, strain rate, rock strength, and frictional regime. Each of these factors, in turn, depend on other parameters. The frictional regime, for example, has been experimentally described by various empirical laws (e.g., rate-and-state friction, velocity-weakening and velocity-strengthening friction) that in turn depend on different parameters such as temperature, composition and hydration (e.g., Di Toro et al., 2011; Dieterich, 1979; Ruina, 1983). These factors controlling frictional instability are difficult to predict even on Earth.

As such, our findings of a non-zero seismogenic thickness on Venus support the hypothesis that Venus could be seismically active at present. However, we cannot make any direct inferences on whether or not Venus is currently experiencing quakes, or how frequent or large they might be, as important parameters such as Venus' lithospheric stress field, rock strength, and frictional regime are currently unknown. For the time being then, any estimates on Venus' seismicity are therefore limited to theoretical scaling approaches between Earth and Venus (Van Zelst et al., 2024) and future modeling studies.

7. Conclusions

We have determined the thermal structure of Venus' lithosphere using both geophysical constraints and geodynamic thermal evolution models. This, in turn, allowed us to estimate the seismogenic thickness of the planet, assuming that the depth of the seismogenic layer can be approximated by the depth of the 600°C isotherm. Taking into account the three approaches studied, we find that the seismogenic thickness typically ranges from 2 to 35 km. A quantitative comparison between the constraints from flexural analyses and our geodynamic model predictions supports the interpretation that large volumes of magmatic intrusions play an important role in Venus' thermal and tectonic evolution. This aligns with the interpretation of Lourenço et al. (2020), introducing the term “plutonic-squishy lid” for a geodynamic regime where lithospheric and surface deformation is largely controlled by the presence of magmatic intrusions.

Our results support the interpretation that Venus could be seismically active today (Van Zelst et al., 2024) and signal that a seismological mission would be an important milestone for Venus space exploration (Garcia et al., 2024; Krishnamoorthy & Bowman, 2023). Until a seismological mission to Venus returns observations of venusquakes, the capabilities of repeat-pass interferometry of upcoming missions will allow for the quantitative measurements of surface deformation (e.g., Smrekar et al., 2022), helping us to better constrain the possible levels of seismicity of Venus.

Data Availability Statement

All data sets and Python routines to create the figures of this paper can be found in Maia et al. (2024). The code used to estimate the lithospheric thermal gradient from elastic thickness constraints is available in Broquet (2022). We use the VenusTopo719 topography data set (Wieczorek, 2015), derived from the Magellan topography (Ford

& Pettengill, 1992), to create the shaded relief maps. The spherical harmonic coefficients of the mantle density anomalies constraints used in this study are available in Maia (2023). The spherical harmonics data sets were analyzed using the open-source package Pyshtools (Wieczorek & Meschede, 2018). All maps were generated using the open-source software PyGMT (Tian et al., 2024; Wessel et al., 2019). The perceptually uniform color maps used in this work are from Crameri (2018).

Acknowledgments

We thank the anonymous reviewers and Laurent Montési for their feedback, which greatly improved our study. This research was supported by the International Space Science Institute (ISSI) in Bern, Switzerland through ISSI International Team project #566: *Seismicity on Venus: Prediction & Detection* led by Iris van Zelst. A.G. acknowledges funding from the Swiss National Science Foundation Postdoc Mobility Grant P500PN_21729, the Center for Space and Habitability (CSH) at the University of Bern, as well as NCCR PlanetS supported by the Swiss National Science Foundation under Grant 51NF40_205606. A.G. and M.P.P. were partially supported by funds from the Jet Propulsion Laboratory, California Institute of Technology, under a contract with the National Aeronautics and Space Administration (80NM0018D0004). B.D. T. is supported by the European Union—NextGenerationEU and by the 2023 STARS Grants Unipd programme HECATE. S.P.N. acknowledges support from the *Airborne Inversion of Rayleigh waves* (AIR) project, funded by the Research Council of Norway basic research program FRIPRO under contract 335903. A.H. is funded by a UK Space Agency Fellowship in Mars Exploration Science under ST/Y005597/1 and under grant number ST/W002523/1. R.R.H. was supported by NASA grants from the High Operating Temperature Technology (80NSSC22K0988) and Rapid Response Research (80NSSC22M0235) programs. R.F.G. acknowledges the support from Centre National d'Études Spatiales under contract APR project VenusGEOX. The authors gratefully acknowledge the scientific support and HPC resources provided by the German Aerospace Center (DLR). The HPC systems CARA and CARO are partially funded by "Saxon State Ministry for Economic Affairs, Labor and Transport," "Ministry of Science and Culture of Lower Saxony," "Federal Ministry for Economic Affairs and Climate Action" of Germany, and "2023 STARS Grants, University of Padua". Open Access funding enabled and organized by Projekt DEAL.

References

- Ágústsson, K., & Flóvenz, Ó. G. (2005). The thickness of the seismogenic crust in Iceland and its implications for geothermal systems. In *Proceedings of the world geothermal congress* (pp. 24–29).
- Albaric, J., Déverchère, J., Petit, C., Perrot, J., & Le Gall, B. (2009). Crustal rheology and depth distribution of earthquakes: Insights from the central and Southern East African rift system. *Tectonophysics*, 468(1–4), 28–41. <https://doi.org/10.1016/j.tecto.2008.05.021>
- Anderson, F. S., & Smrekar, S. E. (2006). Global mapping of crustal and lithospheric thickness on Venus. *Journal of Geophysical Research*, 111(E8). <https://doi.org/10.1029/2004JE002395>
- Armann, M., & Tackley, P. J. (2012). Simulating the thermochemical magmatic and tectonic evolution of Venus's mantle and lithosphere: Two-dimensional models. *Journal of Geophysical Research*, 117(E12). <https://doi.org/10.1029/2012JE004231>
- Banerdt, W. B., Smrekar, S. E., Banfield, D., Giardini, D., Golombek, M., Johnson, C. L., et al. (2020). Initial results from the InSight mission on Mars. *Nature Geoscience*, 13(3), 1–7. <https://doi.org/10.1038/s41561-020-0544-y>
- Bao, X., Lithgow-Bertelloni, C. R., Jackson, M. G., & Romanowicz, B. (2022). On the relative temperatures of Earth's volcanic hotspots and mid-ocean ridges. *Science*, 375(6576), 57–61. <https://doi.org/10.1126/science.abj8944>
- Basilevsky, A. T., & Head, J. W. (2003). The surface of Venus. *Reports on Progress in Physics*, 66(10), 1699–1734. <https://doi.org/10.1088/0034-4885/66/10/r04>
- Beuthe, M. (2008). Thin elastic shells with variable thickness for lithospheric flexure of one-plate planets. *Geophysical Journal International*, 172(2), 817–841. <https://doi.org/10.1111/j.1365-246x.2007.03671.x>
- Bilotti, F., & Suppe, J. (1999). The global distribution of wrinkle ridges on Venus. *Icarus*, 139(1), 137–157. <https://doi.org/10.1006/icar.1999.6092>
- Bjornnes, E., Johnson, B., & Evans, A. (2021). Estimating Venusian thermal conditions using multiring basin morphology. *Nature Astronomy*, 5(5), 498–502. <https://doi.org/10.1038/s41550-020-01289-6>
- Boettcher, M., Hirth, G., & Evans, B. (2007). Olivine friction at the base of oceanic seismogenic zones. *Journal of Geophysical Research*, 112(B1). <https://doi.org/10.1029/2006JB004301>
- Borrelli, M. E., O'Rourke, J. G., Smrekar, S. E., & Ostberg, C. M. (2021). A global survey of lithospheric flexure at steep-sided domical volcanoes on Venus reveals intermediate elastic thicknesses. *Journal of Geophysical Research: Planets*, 126(7), e2020JE006756. <https://doi.org/10.1029/2020JE006756>
- Brissaud, Q., Krishnamoorthy, S., Jackson, J. M., Bowman, D. C., Komjathy, A., Cutts, J. A., et al. (2021). The first detection of an earthquake from a balloon using its acoustic signature. *Geophysical Research Letters*, 48(12), e2021GL093013. <https://doi.org/10.1029/2021GL093013>
- Broquet, A. (2022). AB — ares/Te_HF_conversion: 0.2.3 [Software]. *Zenodo*. <https://doi.org/10.5281/ZENODO.6050262>
- Broquet, A., Wieczorek, M. A., & Fa, W. (2020). Flexure of the lithosphere beneath the north polar cap of Mars: Implications for ice composition and heat flow. *Geophysical Research Letters*, 47(5), e2019GL086746. <https://doi.org/10.1029/2019GL086746>
- Brown, C. D., & Grimm, R. E. (1997). Tessera deformation and the contemporaneous thermal state of the plateau highlands, Venus. *Earth and Planetary Science Letters*, 147(1–4), 1–10. [https://doi.org/10.1016/S0012-821X\(97\)00007-1](https://doi.org/10.1016/S0012-821X(97)00007-1)
- Cascioli, G., Gülcher, A. J. P., Mazarico, E., & Smrekar, S. E. (2025). A spectrum of tectonic processes at coronae on Venus revealed by gravity and topography. *Science Advances*, 11(20), eadt5932. <https://doi.org/10.1126/sciadv.adt5932>
- Chen, W.-P., & Molnar, P. (1983). Focal depths of intracontinental and intraplate earthquakes and their implications for the thermal and mechanical properties of the lithosphere. *Journal of Geophysical Research*, 88(B5), 4183–4214. <https://doi.org/10.1029/JB088iB05p04183>
- Craig, T., Copley, A., & Jackson, J. (2014). A reassessment of outer-rise seismicity and its implications for the mechanics of oceanic lithosphere. *Geophysical Journal International*, 197(1), 63–89. <https://doi.org/10.1093/gji/ggu013>
- Craig, T. J., Copley, A., & Jackson, J. (2012). Thermal and tectonic consequences of India underthrusting Tibet. *Earth and Planetary Science Letters*, 353(354), 231–239. <https://doi.org/10.1016/j.epsl.2012.07.010>
- Craig, T. J., & Jackson, J. A. (2021). Variations in the seismogenic thickness of east Africa. *Journal of Geophysical Research: Solid Earth*, 126(3). <https://doi.org/10.1029/2020jb020754>
- Crameri, F. (2018). Scientific colour maps (4.0.0). *Zenodo*. Retrieved from <https://zenodo.org/record/2649252>
- Crisp, J. A. (1984). Rates of magma emplacement and volcanic output. *Journal of Volcanology and Geothermal Research*, 20(3–4), 177–211. [https://doi.org/10.1016/0377-0273\(84\)90039-8](https://doi.org/10.1016/0377-0273(84)90039-8)
- Davaille, A., Smrekar, S. E., & Tomlinson, S. (2017). Experimental and observational evidence for plume-induced subduction on Venus. *Nature Geoscience*, 10(5), 349–355. <https://doi.org/10.1038/ngeo2928>
- Déverchère, J., Petit, C., Gileva, N., Radziminovitch, N., Melnikova, V., & San'Kov, V. (2001). Depth distribution of earthquakes in the Baikal rift system and its implications for the rheology of the lithosphere. *Geophysical Journal International*, 146(3), 714–730. <https://doi.org/10.1046/j.0956-540x.2001.1484.484.x>
- Dieterich, J. H. (1979). Modeling of rock friction: 1. Experimental results and constitutive equations. *Journal of Geophysical Research*, 84(B5), 2161–2168. <https://doi.org/10.1029/jb084ib05p02161>
- Di Toro, G., Han, R., Hirose, T., De Paola, N., Nielsen, S., Mizoguchi, K., et al. (2011). Fault lubrication during earthquakes. *Nature*, 471(7339), 494–498. <https://doi.org/10.1038/nature09838>
- Edmond, J., & Paterson, M. (1972). Volume changes during the deformation of rocks at high pressures. *International Journal of Rock Mechanics and Mining Sciences & Geomechanics Abstracts*, 9(2), 161–182. [https://doi.org/10.1016/0148-9062\(72\)90019-8](https://doi.org/10.1016/0148-9062(72)90019-8)
- England, P. (2018). On shear stresses, temperatures, and the maximum magnitudes of earthquakes at convergent plate boundaries. *Journal of Geophysical Research: Solid Earth*, 123(8), 7165–7202. <https://doi.org/10.1029/2018jb015907>
- Fagereng, A., & Biggs, J. (2019). New perspectives on “geological strain rates” calculated from both naturally deformed and actively deforming rocks. *Journal of Structural Geology*, 125, 100–110. <https://doi.org/10.1016/j.jsg.2018.10.004>
- Ford, P. G., & Pettengill, G. H. (1992). Venus topography and kilometer-scale slopes. *Journal of Geophysical Research*, 97(E8), 13103–13114. <https://doi.org/10.1029/92JE01085>

- Foster, A., & Nimmo, F. (1996). Comparisons between the rift systems of east Africa, Earth and Beta Regio, Venus. *Earth and Planetary Science Letters*, 143(1), 183–195. [https://doi.org/10.1016/0012-821X\(96\)00146-X](https://doi.org/10.1016/0012-821X(96)00146-X)
- French, S., & Romanowicz, B. (2015). Broad plumes rooted at the base of the Earth's mantle beneath major hotspots. *Nature*, 525(7567), 95–99. <https://doi.org/10.1038/nature14876>
- Garcia, R. F., Van Zelst, I., Kawamura, T., Näsholm, S. P., Horleston, A., Klaasen, S., et al. (2024). Seismic wave detectability on Venus using ground deformation sensors, infrasound sensors on balloons and airglow imagers. *Earth and Space Science*, 11(11). <https://doi.org/10.1029/2024ea003670>
- Ghail, R. (2015). Rheological and petrological implications for a stagnant lid regime on Venus. *Planetary and Space Science*, 113–114, 2–9. <https://doi.org/10.1016/j.pss.2015.02.005>
- Grimm, R. E. (1994). Recent deformation rates on Venus. *Journal of Geophysical Research*, 99(E11), 23163–23171. <https://doi.org/10.1029/94je02196>
- Gülcher, A. J. P., Gerya, T. V., Montési, L. G. J., & Munch, J. (2020). Corona structures driven by plume–lithosphere interactions and evidence for ongoing plume activity on Venus. *Nature Geoscience*, 13(8), 547–554. <https://doi.org/10.1038/s41561-020-0606-1>
- Gülcher, A. J. P., Yu, T.-Y., & Gerya, T. V. (2023). Tectono-magmatic evolution of asymmetric coronae on Venus: Topographic classification and 3D thermo-mechanical modeling. *Journal of Geophysical Research: Planets*, 128(11), e2023JE007978. <https://doi.org/10.1029/2023JE007978>
- Hahn, R. M., & Byrne, P. K. (2023). A morphological and spatial analysis of volcanoes on Venus. *Journal of Geophysical Research: Planets*, 128(4). <https://doi.org/10.1029/2023je007753>
- Herrick, R. R., Bjonnes, E. T., Carter, L. M., Gerya, T., Ghail, R. C., Gillmann, C., et al. (2023). Resurfacing history and volcanic activity of Venus. *Space Science Reviews*, 219(4), 1–32. <https://doi.org/10.1007/s11214-023-00966-y>
- Herrick, R. R., & Hensley, S. (2023). Surface changes observed on a Venusian volcano during the Magellan mission. *Science*, 379(6638), 1205–1208. <https://doi.org/10.1126/science.abm7735>
- Herrick, R. R., & Phillips, R. J. (1992). Geological correlations with the interior density structure of Venus. *Journal of Geophysical Research*, 97(E10), 16017–16034. <https://doi.org/10.1029/92JE01498>
- Hirth, G., & Kohlstedt, D. (2004). Rheology of the upper mantle and the mantle wedge: A view from the experimentalists. In *Inside the subduction factory* (pp. 83–105). American Geophysical Union. <https://doi.org/10.1029/138gm06>
- Hirth, G., & Tullis, J. (1994). The brittle-plastic transition in experimentally deformed quartz aggregates. *Journal of Geophysical Research*, 99(B6), 11731–11747. <https://doi.org/10.1029/93jb02873>
- Hüttig, C., Tosi, N., & Moore, W. B. (2013). An improved formulation of the incompressible Navier-Stokes equations with variable viscosity. *Physics of the Earth and Planetary Interiors*, 40, 113–129. <https://doi.org/10.1016/j.pepi.2013.04.002>
- Ivanov, M. A., & Head, J. W. (2011). Global geological map of Venus. *Planetary and Space Science*, 59(13), 1559–1600. <https://doi.org/10.1016/j.pss.2011.07.008>
- Jackson, D., Jamesand, M. K., Priestley, K., & Emmerson, B. (2008). New views on the structure and rheology of the lithosphere. *Journal of the Geological Society*, 165(2), 453–465. <https://doi.org/10.1144/0016-76492007-109>
- James, P. B., Zuber, M. T., & Phillips, R. J. (2013). Crustal thickness and support of topography on Venus. *Journal of Geophysical Research: Planets*, 118(4), 859–875. <https://doi.org/10.1029/2012JE004237>
- Jimenez-Diaz, A., Ruiz, J., Kirby, J. F., Romeo, I., Tejero, R., & Capote, R. (2015). Lithospheric structure of Venus from gravity and topography. *Icarus*, 260, 215–231. <https://doi.org/10.1016/j.icarus.2015.07.020>
- Karato, S.-i., & Barbot, S. (2018). Dynamics of fault motion and the origin of contrasting tectonic style between Earth and Venus. *Scientific Reports*, 8(1), 1–11. <https://doi.org/10.1038/s41598-018-30174-6>
- Kaula, W. M. (1990). Venus: A contrast in evolution to Earth. *Science*, 247(4947), 1191–1196. <https://doi.org/10.1126/science.247.4947.1191>
- Kiefer, W. S., Richards, M. A., Hager, B. H., & Bills, B. G. (1986). A dynamic model of Venus's gravity field. *Geophysical Research Letters*, 13(1), 14–17. <https://doi.org/10.1029/GL013i001p00014>
- Kohlstedt, D., Evans, B., & Mackwell, S. (1995). Strength of the lithosphere: Constraints imposed by laboratory experiments. *Journal of Geophysical Research*, 100(B9), 17–17602. <https://doi.org/10.1029/95JB01460>
- Kohlstedt, D. L., & Mackwell, S. J. (2009). Strength and deformation of planetary lithospheres. In T. R. Watters & R. A. Schultz (Eds.), *Planetary tectonics* (pp. 397–456). Cambridge University Press. <https://doi.org/10.1017/CBO9780511691645.010>
- Konopliv, A. S., Banerdt, W. B., & Sjogren, W. L. (1999). Venus gravity: 180th degree and order model. *Icarus*, 139(1), 3–18. <https://doi.org/10.1006/icar.1999.6086>
- Kremer, C., Blewitt, G., & Klein, E. C. (2014). A geodetic plate motion and global strain rate model. *Geochemistry, Geophysics, Geosystems*, 15(10), 3849–3889. <https://doi.org/10.1002/2014gc005407>
- Krishnamoorthy, S., & Bowman, D. C. (2023). A “floatilla” of airborne seismometers for Venus. *Geophysical Research Letters*, 50(2), e2022GL100978. <https://doi.org/10.1029/2022GL100978>
- Lebonnois, S., Sugimoto, N., & Gilli, G. (2016). Wave analysis in the atmosphere of Venus below 100-km altitude, simulated by the LMD Venus GCM. *Icarus*, 278, 38–51. <https://doi.org/10.1016/j.icarus.2016.06.004>
- Le Feuvre, M., & Wieczorek, M. A. (2011). Nonuniform cratering of the Moon and a revised crater chronology of the inner Solar System. *Icarus*, 214(1), 1–20. <https://doi.org/10.1016/j.icarus.2011.03.010>
- Lourenço, D. L., & Rozel, A. B. (2023). The past and the future of plate tectonics and other tectonic regimes. In *Dynamics of plate tectonics and mantle convection* (pp. 181–196). Elsevier. <https://doi.org/10.1016/B978-0-323-85733-8.00004-4>
- Lourenço, D. L., Rozel, A. B., Ballmer, M. D., & Tackley, P. J. (2020). Plutonic-squishy lid: A new global tectonic regime generated by intrusive magmatism on Earth-like planets. *Geochemistry, Geophysics, Geosystems*, 21(4), e2019GC008756. <https://doi.org/10.1029/2019GC008756>
- Lourenço, D. L., Rozel, A. B., Gerya, T., & Tackley, P. J. (2018). Efficient cooling of rocky planets by intrusive magmatism. *Nature Geoscience*, 11(5), 322–327. <https://doi.org/10.1038/s41561-018-0094-8>
- Lucazeau, F. (2019). Analysis and mapping of an updated terrestrial heat flow data set. *Geochemistry, Geophysics, Geosystems*, 20(8), 4001–4024. <https://doi.org/10.1029/2019gc008389>
- Mackwell, S. J., Zimmerman, M. E., & Kohlstedt, D. L. (1998). High-temperature deformation of dry diabase with application to tectonics on Venus. *Journal of Geophysical Research*, 103(B1), 975–984. <https://doi.org/10.1029/97JB02671>
- Maia, J. (2023). Dynamic gravity and topography modeling: The Venus case [Dataset]. *Zenodo*. <https://doi.org/10.5281/zenodo.8033151>
- Maia, J., Plesa, A.-C., van Zelst, I., Ghail, R., Gülcher, A. J. P., Panning, M. P., et al. (2024). The seismogenic thickness of Venus [Dataset]. *Zenodo*. <https://doi.org/10.5281/zenodo.13133118>
- Maia, J. S., & Wieczorek, M. A. (2022). Lithospheric structure of Venusian crustal plateaus. *Journal of Geophysical Research: Planets*, 127(2), e2021JE007004. <https://doi.org/10.1029/2021JE007004>

- Maia, J. S., Wiczorek, M. A., & Plesa, A. (2023). The mantle viscosity structure of Venus. *Geophysical Research Letters*, 50(15), e2023GL103847. <https://doi.org/10.1029/2023gl103847>
- McGovern, P. J., & Solomon, S. C. (1997). Filling of flexural moats around large volcanoes on Venus: Implications for volcano structure and global magmatic flux. *Journal of Geophysical Research*, 102(E7), 16303–16318. <https://doi.org/10.1029/97JE01318>
- McKenzie, D., Ford, P., Johnson, C., Parsons, B., Sandwell, D., Saunders, S., & Solomon, S. (1992). Features on Venus generated by plate boundary processes. *Journal of Geophysical Research*, 97(E8), 13533–13544. <https://doi.org/10.1029/92JE01350>
- McKenzie, D., Jackson, J., & Priestley, K. (2005). Thermal structure of oceanic and continental lithosphere. *Earth and Planetary Science Letters*, 233(3–4), 337–349. <https://doi.org/10.1016/j.epsl.2005.02.005>
- McNutt, M. K. (1984). Lithospheric flexure and thermal anomalies. *Journal of Geophysical Research*, 89(B13), 11180–11194. <https://doi.org/10.1029/JB089iB13p11180>
- Molnar, P. (2020). The brittle-plastic transition, earthquakes, temperatures, and strain rates. *Journal of Geophysical Research: Solid Earth*, 125(7), e2019JB019335. <https://doi.org/10.1029/2019JB019335>
- Moore, W. B., & Webb, A. G. (2013). Heat-pipe Earth. *Nature*, 501(7468), 501–505. <https://doi.org/10.1038/nature12473>
- Mueller, S., & Phillips, R. J. (1995). On the reliability of lithospheric constraints derived from models of outer-rise flexure. *Geophysical Journal International*, 123(3), 887–902. <https://doi.org/10.1111/j.1365-246X.1995.tb06896.x>
- Nakagawa, T., & Tackley, P. J. (2012). Influence of magmatism on mantle cooling surface heat flow and Urey ratio. *Earth and Planetary Science Letters*, 329(330), 1–10. <https://doi.org/10.1016/j.epsl.2012.02.011>
- Nimmo, F., & Mackwell, S. (2023). Viscous relaxation as a probe of heat flux and crustal plateau composition on Venus. *Proceedings of the National Academy of Sciences*, 120(3), e2216311120. <https://doi.org/10.1073/pnas.2216311120>
- Ogawa, M., & Yanagisawa, T. (2011). Numerical models of Martian mantle evolution induced by magmatism and solid-state convection beneath stagnant lithosphere. *Journal of Geophysical Research*, 116(E8), E08008. <https://doi.org/10.1029/2010JE003777>
- O'Rourke, J. G., & Smrekar, S. E. (2018). Signatures of lithospheric flexure and elevated heat flow in stereo topography at coronae on Venus. *Journal of Geophysical Research: Planets*, 123(2), 369–389. <https://doi.org/10.1002/2017JE005358>
- Padovan, S., Tosi, N., Plesa, A.-C., & Ruedas, T. (2017). Impact-induced changes in source depth and volume of magmatism on Mercury and their observational signatures. *Nature Communications*, 8(1), 1–10. <https://doi.org/10.1038/s41467-017-01692-0>
- Pauer, M., Fleming, K., & Čadež, O. (2006). Modeling the dynamic component of the geoid and topography of Venus. *Journal of Geophysical Research*, 111(E11). <https://doi.org/10.1029/2005je002511>
- Pfiffner, O. A., & Ramsay, J. G. (1982). Constraints on geological strain rates: Arguments from finite strain states of naturally deformed rocks. *Journal of Geophysical Research*, 87(B1), 311–321. <https://doi.org/10.1029/jb087ib01p00311>
- Phillips, R. J. (1994). Estimating lithospheric properties at Atla Regio, Venus. *Icarus*, 112(1), 147–170. <https://doi.org/10.1006/icar.1994.1175>
- Phillips, R. J., Johnson, C. L., Mackwell, S. J., Morgan, P., Sandwell, D. T., & Zuber, M. T. (1997). Lithospheric mechanics and dynamics of Venus. In S. W. Brougher, D. M. Hunten, & R. J. Phillips (Eds.), *Venus II* (pp. 1163–1204). University of Arizona Press.
- Phillips, R. J., Kaula, W. M., McGill, G. E., & Malin, M. C. (1981). Tectonics and evolution of Venus. *Science*, 212(4497), 879–887. <https://doi.org/10.1126/science.212.4497.879>
- Putirka, K. (2008). Excess temperatures at ocean islands: Implications for mantle layering and convection. *Geology*, 36(4), 283–286. <https://doi.org/10.1130/G24615A.1>
- Regorda, A., Thieulot, C., Van Zelst, I., Erdős, Z., Maia, J., & Buitert, S. (2023). Rifting Venus: Insights from numerical modeling. *Journal of Geophysical Research: Planets*, 128(3), e2022JE007588. <https://doi.org/10.1029/2022JE007588>
- Richards, F., Hoggard, M., Cowton, L., & White, N. (2018). Reassessing the thermal structure of oceanic lithosphere with revised global inventories of basement depths and heat flow measurements. *Journal of Geophysical Research: Solid Earth*, 123(10), 9136–9161. <https://doi.org/10.1029/2018jb015998>
- Richards, M. A., & Hager, B. H. (1984). Geoid anomalies in a dynamic Earth. *Journal of Geophysical Research*, 89(B7), 5987–6002. <https://doi.org/10.1029/JB089iB07p05987>
- Rolf, T., Steinberger, B., Sruthi, U., & Werner, S. (2018). Inferences on the mantle viscosity structure and the post-overturn evolutionary state of Venus. *Icarus*, 313, 107–123. <https://doi.org/10.1016/j.icarus.2018.05.014>
- Rolf, T., Weller, M., Gülcher, A., Byrne, P., O'Rourke, J. G., Herrick, R., et al. (2022). Dynamics and evolution of Venus' mantle through time. *Space Science Reviews*, 218(8), 70. <https://doi.org/10.1007/s11214-022-00937-9>
- Ruina, A. (1983). Slip instability and state variable friction laws. *Journal of Geophysical Research*, 88(B12), 10359–10370. <https://doi.org/10.1029/jb088ib12p10359>
- Russell, M. B., & Johnson, C. L. (2021). Evidence for a locally thinned lithosphere associated with recent volcanism at Aramaiti Corona, Venus. *Journal of Geophysical Research: Planets*, 126(8), e2020JE006783. <https://doi.org/10.1029/2020JE006783>
- Sabbeth, L., Smrekar, S., & Stock, J. (2023). Estimated seismicity of Venusian wrinkle ridges based on fault scaling relationships. *Earth and Planetary Science Letters*, 619, 118308. <https://doi.org/10.1016/j.epsl.2023.118308>
- Sandwell, D. T., & Schubert, G. (1992). Flexural ridges, trenches, and outer rises around coronae on Venus. *Journal of Geophysical Research*, 97(E10), 16069–16083. <https://doi.org/10.1029/92JE01274>
- Schilling, J.-G. (1991). Fluxes and excess temperatures of mantle plumes inferred from their interaction with migrating mid-ocean ridges. *Nature*, 352(6334), 397–403. <https://doi.org/10.1038/352397a0>
- Scholz, C. H. (1988). The brittle-plastic transition and the depth of seismic faulting. *Geologische Rundschau*, 77(1), 319–328. <https://doi.org/10.1007/bf01848693>
- Scholz, C. H. (1998). Earthquakes and friction laws. *Nature*, 391(6662), 37–42. <https://doi.org/10.1038/34097>
- Simons, M., Solomon, S., & Hager, B. (1997). Localization of gravity and topography: Constraints on the tectonics and mantle dynamics of Venus. *Geophysical Journal International*, 131(1), 24–44. <https://doi.org/10.1111/j.1365-246X.1997.tb00593.x>
- Sleep, N. H. (1990). Hotspots and mantle plumes: Some phenomenology. *Journal of Geophysical Research*, 95(B5), 6715–6736. <https://doi.org/10.1029/JB095iB05p06715>
- Smrekar, S., Hensley, S., Nybakken, Mark Wallace, R., Perkovic-Martin, D., You, T.-H., et al. (2022). VERITAS (Venus Emissivity, Radio Science, InSAR, Topography, and Spectroscopy): A discovery mission. In 2022 IEEE Aerospace Conference (AERO). IEEE. <https://doi.org/10.1109/aero53065.2022.9843269>
- Smrekar, S., Stofan, E., Mueller, N., Treiman, A., Elkins-Tanton, L., Helbert, J., et al. (2010). Recent hotspot volcanism on Venus from VIRTIS emissivity data. *Science*, 328(5978), 605–608. <https://doi.org/10.1126/science.11867>
- Smrekar, S. E. (1994). Evidence for active hotspots on Venus from analysis of Magellan gravity data. *Icarus*, 112(1), 2–26. <https://doi.org/10.1006/icar.1994.1166>

- Smrekar, S. E., Kiefer, W. S., & Stofan, E. R. (1997). Large volcanic rises on Venus. In S. W. Bougher, D. M. Hunten, & R. J. Phillips (Eds.) *Venus II* (pp. 845–878). <https://doi.org/10.2307/j.ctv27tct5m.29>
- Smrekar, S. E., Ostberg, C., & O'Rourke, J. G. (2023). Earth-like lithospheric thickness and heat flow on Venus consistent with active rifting. *Nature Geoscience*, 16(1), 13–18. <https://doi.org/10.1038/s41561-022-01068-0>
- Solomon, S. C., & Head, J. W. (1990). Lithospheric flexure beneath the Freyja Montes Foredeep, Venus: Constraints on lithospheric thermal gradient and heat flow. *Geophysical Research Letters*, 17(9), 1393–1396. <https://doi.org/10.1029/GL017i009p01393>
- Steinberger, B., Werner, S. C., & Torsvik, T. H. (2010). Deep versus shallow origin of gravity anomalies, topography and volcanism on Earth, Venus and Mars. *Icarus*, 207(2), 564–577. <https://doi.org/10.1016/j.icarus.2009.12.025>
- Stevenson, D., Cutts, J., Mimoun, D., Arrowsmith, S., Banerdt, B., Blom, P., et al. (2015). *Probing the interior structure of Venus*. (Tech. Rep.). Keck Institute for Space Studies: Venus Seismology Study Team.
- Stixrude, L., de Koker, N., Sun, N., Mookherjee, M., & Karki, B. B. (2009). Thermodynamics of silicate liquids in the deep Earth. *Earth and Planetary Science Letters*, 278(3–4), 226–232. <https://doi.org/10.1016/j.epsl.2008.12.006>
- Stofan, E. R., Sharpton, V. L., Schubert, G., Baer, G., Bindschadler, D. L., Janes, D. M., & Squyres, S. W. (1992). Global distribution and characteristics of coronae and related features on Venus: Implications for origin and relation to mantle processes. *Journal of Geophysical Research*, 97(E8), 13347–13378. <https://doi.org/10.1029/92je01314>
- Stofan, E. R., Smrekar, S. E., Bindschadler, D. L., & Senske, D. A. (1995). Large topographic rises on Venus: Implications for mantle upwelling. *Journal of Geophysical Research*, 100(E11), 23317–23327. <https://doi.org/10.1029/95JE01834>
- Sulcanese, D., Mitri, G., & Mastrogioseppe, M. (2024). Evidence of ongoing volcanic activity on Venus revealed by Magellan radar. *Nature Astronomy*, 8(8), 973–982. <https://doi.org/10.1038/s41550-024-02272-1>
- Surkov, Y. A., Barsukov, V. L., Moskal'yeva, L. P., Kharyukova, V. P., & Kemurdzhian, A. L. (1984). New data on the composition, structure, and properties of Venus rock obtained by Venera 13 and Venera 14. *Journal of Geophysical Research*, 89(B1), 393–402. <https://doi.org/10.1029/JB089iS02p0B393>
- Surkov, Y. A., Moskal'yova, L. P., Kharyukova, V. P., Dudin, A. D., Smirnov, G. G., & Zaitseva, S. Y. (1986). Venus rock composition at the Vega 2 landing site. *Journal of Geophysical Research*, 91(B13), E215–E218. <https://doi.org/10.1029/JB091iB13p0E215>
- Tian, D., Uieda, L., Leong, W. J., Fröhlich, Y., Schlitzer, W., Grund, M., et al. (2024). PyGMT: A Python interface for the Generic Mapping Tools. *Zenodo*. <https://doi.org/10.5281/zenodo.11062720>
- Tian, J., Tackley, P. J., & Lourenço, D. L. (2023). The tectonics and volcanism of Venus: New modes facilitated by realistic crustal rheology and intrusive magmatism. *Icarus*, 399, 115539. <https://doi.org/10.1016/j.icarus.2023.115539>
- Tosi, N., Yuen, D. A., de Koker, N., & Wentzcovitch, R. M. (2013). Mantle dynamics with pressure- and temperature-dependent thermal expansivity and conductivity. *Physics of the Earth and Planetary Interiors*, 217, 48–58. <https://doi.org/10.1016/j.pepi.2013.02.004>
- Tullis, J., & Yund, R. A. (1977). Experimental deformation of dry westerly granite. *Journal of Geophysical Research* (1896–1977), 82(36), 5705–5718. <https://doi.org/10.1029/JB082i036p05705>
- Turcotte, D. L., & Schubert, G. (2002). *Geodynamics*. Cambridge University Press. <https://doi.org/10.1017/CBO9780511843877>
- Turcotte, D. L., Willemann, R. J., Haxby, W. F., & Norberry, J. (1981). Role of membrane stresses in the support of planetary topography. *Journal of Geophysical Research*, 86(B5), 3951–3959. <https://doi.org/10.1029/jb086ib05p03951>
- Uppalapati, S., Rolf, T., Crameri, F., & Werner, S. C. (2020). Dynamics of lithospheric overturns and implications for Venus's surface. *Journal of Geophysical Research: Planets*, 125(11), e2019JE006258. <https://doi.org/10.1029/2019JE006258>
- Van Zelst, I., Maia, J. S., Plesa, A.-C., Ghail, R., & Spühler, M. (2024). Estimates on the possible annual seismicity of Venus. *Journal of Geophysical Research: Planets*, 129(7), e2023JE008048. <https://doi.org/10.1029/2023JE008048>
- Van Zelst, I., Thieulot, C., & Craig, T. J. (2023). The effect of temperature-dependent material properties on simple thermal models of subduction zones. *Solid Earth*, 14(7), 683–707. <https://doi.org/10.5194/se-14-683-2023>
- Violay, M., Gibert, B., Mainprice, D., Evans, B., Dautria, J., Azais, P., & Pezard, P. (2012). An experimental study of the brittle-ductile transition of basalt at oceanic crust pressure and temperature conditions. *Journal of Geophysical Research*, 117(B3). <https://doi.org/10.1029/2011JB008884>
- Voll, G. (1976). Recrystallization of quartz, biotite and feldspars from Erstfeld to the Leventina nappe, Swiss Alps, and its geological significance. *Schweizerische mineralogische und petrographische Mitteilungen*, 56, 641–647.
- Wessel, P., Luis, J. F., Uieda, L., Scharroo, R., Wobbe, F., Smith, W. H. F., & Tian, D. (2019). The generic mapping tools version 6. *Geochemistry, Geophysics, Geosystems*, 20(11), 5556–5564. <https://doi.org/10.1029/2019GC008515>
- White, R., & McKenzie, D. (1995). Mantle plumes and flood basalts. *Journal of Geophysical Research*, 100(B9), 17543–17585. <https://doi.org/10.1029/95jb01585>
- Wieczorek, M. A. (2015). Spherical harmonic model of the planet Venus: Venustopo719 [Dataset]. *Zenodo*. Retrieved from <https://zenodo.org/record/3870926>
- Wieczorek, M. A., & Meschede, M. (2018). SHTools: Tools for working with spherical harmonics. *Geochemistry, Geophysics, Geosystems*, 19(8), 2574–2592. <https://doi.org/10.1029/2018gc007529>
- Zuza, A. V., & Cao, W. (2020). Seismogenic thickness of California: Implications for thermal structure and seismic hazard. *Tectonophysics*, 782–783, 228426. <https://doi.org/10.1016/j.tecto.2020.228426>